



Simulations of the
transport and
deposition of ^{137}Cs
after Chernobyl

N. Evangeliou et al.

This discussion paper is/has been under review for the journal Atmospheric Chemistry and Physics (ACP). Please refer to the corresponding final paper in ACP if available.

Simulations of the transport and deposition of ^{137}Cs over Europe after the Chernobyl NPP accident: influence of varying emission-altitude and model horizontal and vertical resolution

N. Evangeliou¹, Y. Balkanski¹, A. Cozic¹, and A. P. Møller²

¹Laboratoire des Sciences du Climat et de l'Environnement (LSCE), CEA-UVSQ-CNRS, UMR8212, Institut Pierre et Simon Laplace, L'Orme des Merisiers, 91191 Gif sur Yvette Cedex, France

²Laboratoire d'Ecologie, Systématique et Evolution, CNRS UMR8079, Université Paris-Sud, Bâtiment 362, 91405 Orsay Cedex, France

Received: 23 October 2012 – Accepted: 11 March 2013 – Published: 20 March 2013

Correspondence to: N. Evangeliou (nikolaos.evangeliou@lsce.ipsl.fr)

Published by Copernicus Publications on behalf of the European Geosciences Union.

Title Page

Abstract

Introduction

Conclusions

References

Tables

Figures



Back

Close

Full Screen / Esc

Printer-friendly Version

Interactive Discussion



Abstract

The coupled model LMDzORINCA has been used to simulate the transport, wet and dry deposition of the radioactive tracer ^{137}Cs after accidental releases. For that reason, two horizontal resolutions were deployed and used in the model, a regular grid of $2.5^\circ \times 1.25^\circ$, and the same grid stretched over Europe to reach a resolution of $0.45^\circ \times 0.51^\circ$. The vertical dimension is represented with two different resolutions, 19 and 39 levels, respectively, extending up to mesopause. Four different simulations are presented in this work; the first uses the regular grid over 19 vertical levels assuming that the emissions took place at the surface (RG19L(S)), the second also uses the regular grid over 19 vertical levels but realistic source injection heights (RG19L); in the third resolution the grid is regular and the vertical resolution 39 vertical levels (RG39L) and finally, it is extended to the stretched grid with 19 vertical levels (Z19L). The best choice for the model validation was the Chernobyl accident which occurred in Ukraine (ex-USSR) on 26 May 1986. This accident has been widely studied since 1986, and a large database has been created containing measurements of atmospheric activity concentration and total cumulative deposition for ^{137}Cs from most of the European countries.

According to the results, the performance of the model to predict the transport and deposition of the radioactive tracer was efficient and accurate presenting low biases in activity concentrations and deposition inventories, despite the large uncertainties on the intensity of the source released. However, the best agreement with observations was obtained using the highest horizontal resolution of the model (Z19L run). The model managed to predict the radioactive contamination in most of the European regions (similar to Atlas), and also the arrival times of the radioactive fallout. As regards to the vertical resolution, the largest biases were obtained for the 39 layers run due to the increase of the levels in conjunction with the uncertainty of the source term. Moreover, the ecological half-life of ^{137}Cs in the atmosphere after the accident ranged between 6 and 9 days, which is in good accordance to what previously reported and in the same

ACPD

13, 7681–7736, 2013

Simulations of the transport and deposition of ^{137}Cs after Chernobyl

N. Evangeliou et al.

Title Page

Abstract

Introduction

Conclusions

References

Tables

Figures

⏪

⏩

◀

▶

Back

Close

Full Screen / Esc

Printer-friendly Version

Interactive Discussion

range with the recent accident in Japan. The high response of LMDzORINCA model for ^{137}Cs reinforces the importance of atmospheric modeling in emergency cases to gather information for protecting the population from the adverse effects of radiation.

1 Introduction

The Chernobyl Nuclear Power Plant (NPP) accident on 26 April 1986 resulted in the dispersion and deposition of a large amount of radionuclides into the environment. On 26 April 1986, two explosions took place in the power plant releasing and transporting radioactive materials over long distances. The absence of reliable models in the period of the accident and the lack of reliable information on the direction taken by the released elements motivated several researchers to develop environmental modeling tools, in order to be able to study potential accidental scenarios. Since then, many national and international efforts have been initiated to develop reliable models that will be able to describe transport and dispersion mechanisms when large amounts of radionuclides are released. Such tracer models can be used to estimate the spatiotemporal distribution of the fallout from accidental releases and the output can be used for preventive purposes, as well as to estimate the exposure and the harmful impacts from the dangerous compounds on humans, animals and vegetation.

It has been estimated that over 10 EBq ($\times 10^{18}\text{ Bq}$) of fission and activation products escaped from the damaged reactor (De Cort et al., 1998), whereas 2 EBq (the most refractory) were deposited in the 30 km vicinity of the power plant (Hatano et al., 1998). The most abundant nuclides were ^{133}Xe ($\sim 6500\text{ PBq}$), ^{131}I ($1200\text{--}1700\text{ PBq}$), ^{132}Te ($1000\text{--}1200\text{ PBq}$), ^{137}Cs ($\sim 85\text{ PBq}$), ^{90}Sr (81 PBq), ^{134}Cs ($44\text{--}48\text{ PBq}$), whereas the most refractory, less volatile radionuclides were ^{144}Ce , ^{141}Ce , ^{106}Ru , ^{140}Ba , ^{95}Zr , ^{99}Mo , $^{238\text{--}241}\text{Pu}$ etc. (Devell et al., 1996; De Cort et al., 1998). However, a radionuclide of major concern is ^{137}Cs , due to its half-life (30.2 y), the radiation type it emits during its radioactive decay and its bioaccumulation by organisms. Consequently, it is a chemical analogue of potassium and rubidium with high mobility in biological

Simulations of the transport and deposition of ^{137}Cs after Chernobyl

N. Evangeliou et al.

Title Page

Abstract

Introduction

Conclusions

References

Tables

Figures

⏪

⏩

◀

▶

Back

Close

Full Screen / Esc

Printer-friendly Version

Interactive Discussion



Simulations of the transport and deposition of ^{137}Cs after Chernobyl

N. Evangeliou et al.

Title Page

Abstract

Introduction

Conclusions

References

Tables

Figures

⏪

⏩

◀

▶

Back

Close

Full Screen / Esc

Printer-friendly Version

Interactive Discussion

systems. Its chemical and metabolic-physiological reactions are similar to those of potassium (Woodhead, 1973) that is essential for many organisms. This explains why ^{137}Cs gets enriched within tissues and cells. However, Cs cannot easily replace K in its metabolic functions, and it is not usually received by organisms in the same portion as potassium (Kornberg, 1961). Finally, it also participates in the augmentation of the total radioactivity to which the population is exposed.

Despite the dramatic consequences of the Chernobyl reactor accident, the atmospheric releases and the observed deposition of radionuclides provide a challenge for the modelers to test and improve their long-range dispersion models. For many years, operational codes have been developed to quantify the global fluxes of chemical pollutants (Elliassen, 1978; Elliassen and Saltbones, 1983; Prather et al., 1987; Lee et al., 2001; Stier et al., 2005; Koch et al., 2009; Huneus et al., 2011; Olivié et al., 2012 and many others). At the same time, some authors proposed the use of certain codes to analyse and/or predict the atmospheric transfer of radionuclides (ApSimon et al., 1985; ApSimon et al., 1987; Jacob et al., 1987; Albergel et al., 1988; Lange et al., 1988; Hass et al., 1990; Piedelievre et al., 1990; Balkanski et al., 1992; Klug et al., 1992; Ishikawa, 1995; Jacob et al., 1997; Brandt et al., 2002). It is well established that such models provide a good description of the climatological long-range transport. However, the inconvenience in such studies arises from the fact that the simulations of the pollution episodes cannot be easily validated due to the lack of real-time qualitative measurements.

Many simulational studies have been performed in order to predict how the radioactive ^{137}Cs migrated after the accident (e.g. Alberger et al., 1988; Hass et al., 1990; Bonelli et al., 1992; Desiato, 1992; Salvadori et al., 1996; Hatano et al., 1998; Brandt et al., 2002). The primary subject of these studies was emergency evacuation planning over regions within 30 km from the site (called “the exclusion zone”), although most of the results were proven to be inconsistent with the measured data obtained afterwards. Today, more than 25 years after the date of the accident, a better understanding of the fate of radionuclides has been obtained in terms of total deposition. Furthermore,

Simulations of the transport and deposition of ^{137}Cs after Chernobyl

N. Evangeliou et al.

Title Page

Abstract

Introduction

Conclusions

References

Tables

Figures

⏪

⏩

◀

▶

Back

Close

Full Screen / Esc

Printer-friendly Version

Interactive Discussion

high quality deposition measurements over Europe have become available from the Chernobyl period by the EU Joint Research Centre (JRC) called “the REM database”, whereas high resolution maps have been created called “Atlas of caesium deposition on Europe after the Chernobyl accident” (De Cort et al., 1998). These data have being continuously collected by the EU since 1986 in the frame of the REM (Radioactivity Environmental Monitoring) project presenting atmospheric activity concentrations and deposition inventories from European countries, and then used in this paper to validate the model ability to represent the spread and deposition of ^{137}Cs . For the creation of the map (hereafter, referred to as the Atlas), the data have been corrected for radioactive decay to 10 May 1986. A similar map has also been published by Peplow (2006).

Consequently, the main goal of the present work was to study the efficiency of the model described here for the tracer ^{137}Cs using the already known patterns of the Chernobyl releases and transportation over Europe. Therefore, (i) the altitude of the emissions after the episode was considered assuming that the emissions occurred (a) at the surface and (b) at several heights. Moreover, the resulting dispersion and deposition of ^{137}Cs is presented using (ii) the regular grid ($2.5^\circ \times 1.25^\circ$) and (iii) the zoom-version of the model. Finally, the results of the two versions are evaluated by using two different vertical resolutions: 19 and 39 vertical layers for the regular grid configuration. All the results have been compared with raw data from the REM database. Given the large global risk of human exposure to radiation, especially in areas around reactors in densely populated regions, notably in West Europe and South Asia, where a major reactor accident can expose around 30 million people to radioactive contamination (Lelieveld et al., 2012), a reliable transport model for radioactive substances would be a benefit. The recent decision by Germany (following the Fukushima Daiichi accident in Japan) to phase out its nuclear reactors will reduce the national risk, though a large risk will still remain from the reactors in the neighbouring countries.

2 Global atmospheric transport model

The aerosol module INCA (INteractions between Chemistry and Aerosols) is coupled to the general circulation model (GCM), LMDz, developed at the Laboratoire de Météorologie Dynamique in Paris, and the global vegetation model ORCHIDEE (ORganizing Carbon and Hydrology In Dynamic Ecosystems Environment) (LMDzORINCA) (see also Szopa et al., 2012). The gas phase chemistry part in the model is described by Hauglustaine et al. (2004). Aerosols and gases are treated in the same code to ensure coherence between gas phase chemistry and aerosol dynamics as well as possible interactions between gases and aerosol particles. The simulations using the regular grid described below were performed with a maximum horizontal resolution of 2.5 degrees in longitude and 1.25 degrees in latitude (144 × 142) (Fig. 1a). However, the GCM also offers the possibility to zoom over specific regions by stretching the grid with the same number of gridboxes (Fig. 1b). In the present study the zoom version was used in Europe obtaining a maximum horizontal resolution of 0.45 degrees in longitude and 0.51 degrees in latitude. On the vertical plane, the model uses sigma-p coordinates with 19 levels extending from the surface up to about 3.8 hPa corresponding to a vertical resolution of about 300–500 m in the planetary boundary layer (first level at 70 m height) and to a resolution of about 2 km at the tropopause (with 7–9 levels located in the stratosphere). Moreover, a vertical resolution of 39 layers has been installed and used extending from the surface up to the mesopause.

Each simulation was carried out for nine months (April to December 1986). Deposition of ^{137}Cs in Europe one month after Chernobyl appeared to be at least two orders of magnitude, or more, lower than the maximum deposition just after the accident, and also that it was fractional (below detection limit) one year later (Kritidis, 1989). Therefore, nine months were sufficient to obtain more than 99 % of the ^{137}Cs emitted. LMDzORINCA accounts for emissions, transport (resolved and sub-grid scale), photochemical transformations, and scavenging (dry deposition and washout) of chemical species and aerosols interactively in the GCM. Several versions of the INCA model are

ACPD

13, 7681–7736, 2013

Simulations of the transport and deposition of ^{137}Cs after Chernobyl

N. Evangeliou et al.

Title Page

Abstract

Introduction

Conclusions

References

Tables

Figures

⏪

⏩

◀

▶

Back

Close

Full Screen / Esc

Printer-friendly Version

Interactive Discussion

currently available depending on the envisaged applications with the chemistry-climate model. The model can be run in a nudged mode, relaxing to ECMWF (European Centre for Medium-Range Weather Forecasts) meteorology (Hourdin and Issartel, 2000).

The radioactive tracer ^{137}Cs (half-life = 30.2 yr) was inserted as an inert tracer within the model. The behaviour of ^{137}Cs in the atmosphere is strongly related to its chemical form as it may be released in the atmosphere in gaseous form or adsorbed onto particles. Here, it is assumed that mostly ^{137}Cs behaves as an aerosol and as such it is treated in the model. In fact, this is true as it has been reported that over 80 % of the ^{137}Cs emitted in the atmosphere during accidental releases is in the form of particulates (Morino et al., 2011; Richie and McHenry, 1990; Potiriadis et al., 2011; Sportisse, 2007; Yoschenko et al., 2006). The partitioning between gaseous form and particles and the size distribution of aerosols strongly affect dry deposition and scavenging.

3 Emission estimates after the accident

The coordinates of the emissions after the Chernobyl accident in the model were set to 30.083° E longitude and 51.383° N latitude. The precise amount of the emissions after the accident is still laden with uncertainty for the researchers and the local authorities and, typically, an uncertainty of 50 % is used in such analyses (e.g. Albeger et al., 1988; Hass et al., 1990; Brandt et al., 2002). The total source term evaluated by the ex-USSR authorities and published at an IAEA conference in 1986 (Hass et al., 1990) presented a value of 37 ($\pm 50\%$) PBq for ^{137}Cs estimated on the basis that all the emitted ^{137}Cs had been deposited in ex-USSR countries only. Nevertheless, a subsequent estimation of the activity of ^{137}Cs emitted after the accident, taking into account the amount of ^{137}Cs deposited in all countries, showed a value more than 2 times higher ($85 \pm 50\%$ PBq), which is 30 % of the total core inventory of ^{137}Cs (280 PBq) (IAEA, 2006). The daily emission percentages (with respect to the total release) have been estimated to be: 24 % for 26 April, 8 % for 27 April, 6.8 % for 28 April, 5.2 % for 29 April, 4 % for 30 April, 4 % for 1 May, 8 % for 2 May, 10 % for 3 May, 14 % for 4 May, 16 %

Simulations of the transport and deposition of ^{137}Cs after Chernobyl

N. Evangeliou et al.

Title Page

Abstract

Introduction

Conclusions

References

Tables

Figures

⏪

⏩

◀

▶

Back

Close

Full Screen / Esc

Printer-friendly Version

Interactive Discussion



Simulations of the transport and deposition of ^{137}Cs after Chernobyl

N. Evangeliou et al.

Title Page

Abstract

Introduction

Conclusions

References

Tables

Figures

⏪

⏩

◀

▶

Back

Close

Full Screen / Esc

Printer-friendly Version

Interactive Discussion

for 5 May, whereas on 6 May emitted quantities were 3 to 4 orders of magnitude lower. The respective activities and the injection height over 19 and 39 vertical layers can be found in Table 1. The major part of the initial emissions from Chernobyl has been estimated to take place at relatively high altitudes. After a few days, the major parts of the emissions were released at lower altitudes below 1.5 km, and in the following days the concentrations were transported over most of Europe with major influences in southern, eastern and central Europe. As a result of the two explosions held during the first day of the accident, the initial large release was due to the mechanical fragmentation of the fuel. It mainly contained the more volatile radionuclides such as noble gases, iodine and some caesium. The second large release in the end of this period was caused by the high temperatures reached in the core melt (Waight et al., 1995).

4 Parameterisation of wet and dry deposition

The deposition of an atmospheric constituent over a given terrain depends on the local wind speed, the sensible heat, the land-use data (vegetation type, water, soil, etc.), the characteristics of the compound (as, e.g. whether it is in gaseous or in particulate form, or both) and on precipitation (cloud physics). Deposition is defined as the amount of the air pollutant (in both forms), that is transferred to the earth's surface by wet and dry removal processes. It is a time dependent process and varies with meteorological conditions and precipitation. In the present study, ^{137}Cs was assumed to be in particulate form, when released from the nuclear power plant, although the particle size was uncertain, ranging between 0.01 and 50 μm , (Valkama and Pollanen, 1996), and as soluble gas in wet scavenging.

The LMDz general circulation model distinguishes between stratiform and convective precipitation. The wet scavenging of the soluble species (such as cesium) is calculated in INCA for both types of precipitation separately and parameterized as a first-order loss process (Giorgi and Chameides, 1985):

$$\frac{d}{dt}C_g = -\beta C_g \quad (1)$$

where C_g is the gas phase concentration of the considered species and β the scavenging coefficient (1 s^{-1}). The scavenging associated with large-scale stratiform precipitation is calculated adopting the falling raindrop approach and calculating the amount of gas removed by the drop falling through each model layer located below the cloud level (Seinfeld and Pandis, 1998). The increase of the aqueous phase concentration C_{aq}^m of an irreversibly scavenged gas in a droplet originating from level m and falling through a model layer i (where layer $i < \text{layer } m$) can be estimated by a mass balance between the rate of increase of the mass of species in the droplet and the rate of transfer of species to the drop (Seinfeld and Pandis, 1998):

$$\left[\frac{d}{dt}C_{\text{aq}}^m \right]_i = \frac{6K_c}{D_p} C_g^i \quad (2)$$

where C_g^i is the gas phase concentration in layer i encountered by the drop originating from level m , D_p is the rain droplet diameter fixed to a constant value of 3×10^{-3} m in this version of INCA, and K_c the mass transfer coefficient (m s^{-1}). The mass transfer is calculated until equilibrium of the dissolved gas is eventually reached in the falling drop. K_c is calculated with the relation given by Brasseur et al. (1998). In this relation, we assume a constant value for the drop terminal velocity, we assume that rainout is suppressed at temperatures below 258 K.

The scavenging by convective precipitation is calculated as part of the upward convective mass flux on the basis of a modified version of the scheme proposed by Balkanski et al. (1993). On the basis of this formulation and on the basis of Eq. (1), it can be derived, for the scavenging coefficient associated with convective precipitation,

$$\beta^{\text{cv}} = -fF_u \frac{g}{p} \quad (3)$$

Simulations of the transport and deposition of ^{137}Cs after Chernobyl

N. Evangeliou et al.

Title Page

Abstract

Introduction

Conclusions

References

Tables

Figures

◀

▶

◀

▶

Back

Close

Full Screen / Esc

Printer-friendly Version

Interactive Discussion



where f is the fraction of soluble gas removed from the gas phase, F_u the upward convective mass flux diagnosed by the GCM ($\text{kg m}^{-2} \text{s}^{-1}$), p the pressure and g the gravity constant.

As in the study by Liu et al. (2001), we assume that in the convective column,

$$f = 1 - e^{-a\Delta z} \quad (4)$$

where Δz (m) is the height in the convective tower calculated from the cloud base. The scavenging efficiency a (m^{-1}) is calculated as the ratio of the rate constant for conversion of cloud water to precipitation (C_{pr}) and the updraft velocity w . On the basis of Mari et al. (2000) and Liu et al. (2001), we adopt $C_{pr} = 5 \times 10^{-3} \text{ s}^{-1}$, $w = 10 \text{ m s}^{-1}$

leading to $a = 5 \times 10^{-4} \text{ m}^{-1}$.

The dry deposition of ^{137}Cs was computed using the analogy of surface resistance. The deposition velocity is defined as the inverse of the sum of an aerodynamic resistance and a surface resistance placed in series (Balkanski et al., 1993). They are calculated by the following equation:

$$V_d = \frac{1}{R_a + R_b + R_c} \quad (5)$$

where R_a , R_b and R_c (s m^{-1}) are the aerodynamical, quasi-laminar, and surface resistances, respectively. R_a and R_b are calculated on the basis of Walcek et al. (1986). The surface resistances are determined for all species included in LMDZORINCA according to their Henry law equilibrium constant and reactivity factor for oxidation of biological substances. The surface resistances are calculated using the vegetation map classification from De Fries and Townshend (1994) interpolated to the model grid and redistributed into the classification proposed by Wesely (1989). The lower and upper canopy resistances (including stomata, mesophyll, and cuticle resistances) as well as ground resistances are all parameterised according to Wesely (1989). Meteorological variables needed to calculate R_a , R_b and R_c (including temperature, specific humidity,

Simulations of the transport and deposition of ^{137}Cs after Chernobyl

N. Evangeliou et al.

Title Page

Abstract

Introduction

Conclusions

References

Tables

Figures

⏪

⏩

◀

▶

Back

Close

Full Screen / Esc

Printer-friendly Version

Interactive Discussion



wind speed, precipitation, snow cover, and solar radiation at the surface) are provided by the GCM at each time step. The deposition velocities used in the model for that restricted study area (Europe, 10° W–80° E, 25°–75° N) ranged between 0.05 cm s⁻¹ over ocean and 0.2 cm s⁻¹ over land depending on the period of study. These values are within the range of deposition velocities used in such studies, e.g. 0.1 cm s⁻¹ (Hanna, 1991), 0.1–0.5 cm s⁻¹ (Klug et al., 1992) and 0.1 cm s⁻¹ (Hwang et al., 2003).

5 Results and discussion

5.1 Fallout transport over Europe using different model versions

An essential question in the present simulation was how the altitude of the emission affects the transport of ¹³⁷Cs. Therefore, three separate simulations in the regular grid version of the model were performed, the first one assuming that all the amount of ¹³⁷Cs was introduced at the site's surface (RG19L(S)), the second following the real emission altitude according to Table 1 spread over 19 layers (RG19L) and the final one over 39 layer resolution following the same emission patterns (RG39L). Moreover, one additional run was performed after installing the zoom-version of the model, stretched over Europe gridded within 19 vertical layers (Z19L) using the emissions denoted in Table 1. The ¹³⁷Cs activity concentrations in Figs. 2–5 are expressed in Bq (m⁻³ STP), where m³ STP is a standard cubic meter of air at 273.15 K and 1 atm.

The atmospheric activity concentrations of ¹³⁷Cs from the first run (RG19L(S)) are illustrated in Fig. 2 for the first day of the accident (26 March 1986), for the end of March (30 April 1986), as well as for 5 and 10 May 1986, in order to assess the direction of the radioactive fallout. It is noteworthy that the direction of the radioactive fallout seems not to vary much, mostly affecting the southern countries of Europe and the regions located in northern Africa. The atmospheric burden of ¹³⁷Cs was found to be maximum on the last day of the emission (5 May) reaching 24 PBq, which corresponds to 28 % of the total emitted (Table 2), and then decreased exponentially, presenting an ecological

Title Page

Abstract

Introduction

Conclusions

References

Tables

Figures

⏪

⏩

◀

▶

Back

Close

Full Screen / Esc

Printer-friendly Version

Interactive Discussion

at 54 PBq (64 %) on 5 May, while the next months decreased exponentially reaching 0.13 PBq (0.15 %) at the end of 1986.

The same simulation for the Chernobyl accident was performed, after setting up a zoom-version of the model for 19 vertical layers (Z19L), centred over Europe. The initial transport (26 April) of the radioactive fallout shows a more pronounced meridional axis than in the previous simulations directed towards West-central Belarus (north), while a much weaker amount of ^{137}Cs (more than two orders of magnitude less) was transferred to Romania and the Black Sea (south) (Fig. 5). The same transport trends have been validated and reported elsewhere (e.g. Brandt et al., 2002; Hass et al., 1990). At the end of April the three different directions of the plume (north, west, north-eastern) were apparent and the respective levels were similar to the regular grid runs. On 5 May (last day of the emissions), the plume seems more intense in areas close to the source presenting a more local-based transport, with the fallout extending mostly to the east. ^{137}Cs affects the central and eastern European regions, while it has not been transferred to Spain, Portugal and the North-east African countries yet. Observations support this transport pattern as these countries have reported trace amounts of ^{137}Cs activity concentrations in the air or they were below the respective detection limits. The remaining ^{137}Cs (burden) was maximum on 5 May as it was estimated to be 43 PBq in the atmosphere, which corresponds to 51 % of the direct total emission (Table 2). The ecological half-life of ^{137}Cs was also estimated to be almost 6 days (Fig. 6), which is comparable to those estimated by the previous runs and similar to those reported previously for the Chernobyl accident. However, a recent study following the Fukushima NPP accident in Japan showed ecological half-lives of ^{137}Cs to be between 5 and 10 days (Kristiansen et al., 2012). Until 10 May the fallout appeared to follow a southern direction affecting the Middle East, just as in the previous simulations. During the last two thirds of May the radioactive plume over Europe was of the order mBq m^{-3} STP, whereas at the end of the month only 8.2 % (7.0 PBq) of the ^{137}Cs emitted still resided into atmosphere. Likewise, ^{137}Cs decreased in the following months and more than 99.9 % had been deposited by the end of 1986 (Table 2).

Simulations of the transport and deposition of ^{137}Cs after Chernobyl

N. Evangeliou et al.

Title Page

Abstract

Introduction

Conclusions

References

Tables

Figures



Back

Close

Full Screen / Esc

Printer-friendly Version

Interactive Discussion



(c) South Europe. Time series measurements of ^{137}Cs atmospheric concentrations between April and May 1986 can be found in Figs. 8–10 for some of the regions examined. Other stations can be found in the supplementary data of this study.

In West-central Europe (Germany, France, UK, Belgium, Switzerland, Austria and Netherlands), the trends of ^{137}Cs dispersion in the countries examined showed satisfactory results, in terms of activity concentrations and residence times as well (Fig. 8). However, relatively small inaccuracies were observed on some days (e.g. in Austria and Switzerland). The averaging of the measurements does not allow seeing accurately the timing of the rise and falling in activities (with some exceptions). Moreover, the precision of the measurement technique used is not indicated in the database. Data from the REM database have been collected using several different techniques (e.g. direct airborne gamma spectrometry, surface pumping through disc filters followed by gamma spectrometry etc.) and the specific method used at each station is not specified in the database. It should be stated that determination recoveries contrast between different methodologies and this might induce additional uncertainties to the results. Regarding the residence time of ^{137}Cs in the countries presented here, the model also shows robustness since, in most of the cases, similar levels were observed. Finally, the ending dates of the fallout, where ^{137}Cs activity concentrations were near the limit of detection (LOD), concur with those of the model.

Similar results were found for the countries of North Europe (Finland, Norway, Sweden and Denmark) with smaller discrepancies (Fig. 9). The most apparent were observed for Finland and Norway during the first days of May 1986, where the model underestimates the activity concentrations of ^{137}Cs . However, the patterns of ^{137}Cs activity concentrations in all cases were undoubtedly consistent indicating high accuracy for the model. Very similar levels were observed for the starting and the ending point of the radionuclide passage over the countries studied.

Finally, reliable results were obtained for South European countries (ex-Czechoslovakia, Hungary, Italy and Greece) (Fig. 10), albeit underestimations over the Italian territory and overestimations over Greece. It is also essential to focus on

Simulations of the transport and deposition of ^{137}Cs after Chernobyl

N. Evangeliou et al.

Title Page

Abstract

Introduction

Conclusions

References

Tables

Figures

⏪

⏩

◀

▶

Back

Close

Full Screen / Esc

Printer-friendly Version

Interactive Discussion

Simulations of the transport and deposition of ^{137}Cs after Chernobyl

N. Evangeliou et al.

Title Page

Abstract

Introduction

Conclusions

References

Tables

Figures

⏪

⏩

◀

▶

Back

Close

Full Screen / Esc

Printer-friendly Version

Interactive Discussion

another source of uncertainty. Even nowadays the exact emissions from the Chernobyl accident are unknown. Therefore, the relatively large discrepancy in the dosages of ^{137}Cs can be explained from discrepancies in the source term or uncertainties in the effective release heights, since the injection altitudes used in the present study are only educated guesses. This seems to be very essential in terms of transport and deposition of ^{137}Cs in certain regions. Another noteworthy point that we should focus on here is what we learn from the results of the RG19L(S) simulation, where surface emissions were assumed. These results differ significantly from measurements and also model-versions where real emission altitudes were used. For instance, no ^{137}Cs was detected in North Europe until the end of May or extreme amount were estimated in South Europe at the start of the same month. This is additional evidence of how the exact height of the emission could affect the subsequent transport of ^{137}Cs and the importance of the uncertainty induced by the source term.

There are several numerical measures that quantify the extent of statistical dependence between pairs of databases. Here, we used the Spearman correlation method (Choi, 1977), which assesses how well the relationship between two variables can be described using a monotonic function. If there are no repeated data values, a perfect Spearman correlation of +1 or -1 occurs when each of the variables is a perfect monotone function of the other. Table 3 shows the respective results of the datasets compared (REM versus RG19L(S), RG19L, RG39L and Z19L, respectively) for the activity concentrations of ^{137}Cs . According to the table, the Spearman correlation coefficient ranged from 0.61 to 0.64 for the runs where the emission altitude was taken into account for 95 % confident level, whereas it was 0.21 for the RG19L(S) run; thus the variables are statistically dependent. On the other hand, the data of the simulation with the real emission altitude are also highly dependent presenting coefficients of 0.81. For justification, Kendall rank correlation coefficient, commonly referred as Kendall's tau (τ) coefficient (Christensen, 2005) was also estimated (Table 3). This statistic measures the rank correlation, i.e. the similarity of the orderings of the data when ranked by each of the quantities. It is often used to test a statistical hypothesis in order to establish

Simulations of the transport and deposition of ^{137}Cs after Chernobyl

N. Evangeliou et al.

Title Page

Abstract

Introduction

Conclusions

References

Tables

Figures

⏪

⏩

◀

▶

Back

Close

Full Screen / Esc

Printer-friendly Version

Interactive Discussion



whether two variables may be regarded as statistically dependent. This test is non-parametric, as it does not rely on any assumptions on the distributions of X or Y . Under a “null hypothesis” of X and Y being independent, the sampling distribution of τ will have an expected value of zero. Here, the τ values were estimated to be around 0.44 for 95 % confident level; thus, the “null hypothesis” can be rejected and the two datasets are dependent. The data derived from each simulation were very similar with τ coefficients between 0.54–0.68. This can also be seen in Fig. 11, which depicts the Box and Whisker plot of the data. The range of the datasets for ^{137}Cs activity concentrations is very similar, whereas the boxes corresponding to 25–75 % of the values were found at same level, although in some cases the model was found to underestimate. Besides statistics, the average relative biases were also calculated and presented in Figs. 8–10 for each version except the one where surface emissions assumed. Despite the large variation in the biases, they present very satisfactory averages, 9.59, 81.49 and 3.81 for the RG19L, RG39L and Z19L run respectively, which are very good in comparison with previously reported ones for ^{137}Cs activity concentrations of the Chernobyl accident (e.g. –61 in Brandt et al., 2002). The larger positive biases calculated for the 39 levels are a result of the elevation of higher amounts of ^{137}Cs at greater heights (previously discussed in the manuscript) in conjunction with the resulting larger residence times.

Finally, the arrival times of the radioactive fallout of ^{137}Cs were assessed for the four different simulations (RG19L(S), RG19L, RG39L and Z19L) and they were compared to those obtained from the REM database (REM). As arrival time we define the time after the accident it takes for ^{137}Cs to reach the activity concentration of $10^{-4} \text{ Bq m}^{-3}$ in a specific location, which is the minimum detected value of the REM database. The results are illustrated in a scatter plot in Fig. 12 for 56 measurement stations in 24 European countries (Ukraine, Russia, Poland, Romania, Hungary, Denmark, Belgium, Finland, Norway, Sweden, Germany, Netherlands, France, Italy, Great Britain, Austria, Switzerland, ex-Czechoslovakia, Turkey, Greece, Ireland, Egypt, Syria and Lebanon). The Pearson linear correlation coefficient was estimated to be 0.65 for the RG19L run,

0.46 for the RG19L and 0.63 for the Z19L, which is considered to be significant. The different vertical resolution resulted in a more rapid transport to the places examined. Moreover, as in the previous comparisons, the respective arrival times of ^{137}Cs estimated from the regular grid run assuming surface emissions (RG19L(S)) were not reliable ($R^2 = 0.08$). The model is able to predict the arrival times of ^{137}Cs for the measurement stations with a good accuracy.

5.3 Deposition of ^{137}Cs in European countries in relation to the Atlas

In this section the atmospheric budget and deposition patterns of ^{137}Cs are assessed taking into consideration the contributions of different removal processes (i.e. particle sedimentation, dry and wet deposition, through large-scale and convective precipitation). The distribution of ^{137}Cs deposited over Europe is shown in Fig. 13 (for the RG19L(S)), whereas in Fig. 14 the Atlas map is illustrated. Figures 15–17 depict the respective runs with the real emission altitude (RG19L, RG39L and Z19L) for dry (top left panel), wet (top right panel) and total cumulative deposition (lower panel). In these figures, the same scale with the Atlas was used in order to better compare the results. Following the definition given by the International Atomic Energy Agency (IAEA, 2005, 2009), any area with activity larger than 40 kBq m^{-2} is considered to be contaminated (see relevant red scale). Contamination means the presence of a radionuclide on a surface in quantities larger than 40 kBq m^{-2} for beta and gamma emitters (^{137}Cs is a gamma emitter). Since we integrate the deposition over the period after the accident until the end of 1986, the present results represent the cumulated contamination of this radionuclide.

Consequently, the cumulative dry, wet and total deposition for 1986, estimated assuming that the emissions occurred at the surface (RG19L(S)), are depicted in Fig. 13. These data are briefly presented here in order to certify and record the importance of the altitude of the emission in deposition after accidental releases. As can be seen from Fig. 13 the deposition of ^{137}Cs is largely dependent upon the transport of the atmospheric burden. In the present situation where surface emissions assumed, the

Simulations of the transport and deposition of ^{137}Cs after Chernobyl

N. Evangeliou et al.

Title Page

Abstract

Introduction

Conclusions

References

Tables

Figures

⏪

⏩

◀

▶

Back

Close

Full Screen / Esc

Printer-friendly Version

Interactive Discussion

deposition appeared to be a local event. It is mainly contingent from the surface southern winds and, following the dominant precipitation, it was deposited in Eastern Europe and the Balkan countries (Russia, Belarus, and Ukraine, ex-Czechoslovakia, Romania, Bulgaria, Greece and ex-Yugoslavia). An example can be given for Kiev (Ukraine), which is the most densely populated city close to the damaged reactor (< 100 km). According to the Atlas (Fig. 14), the deposition of ^{137}Cs in this location appeared to be of the order of $10\text{--}40\text{ kBq m}^{-3}$. However, the model predicted a deposition greater than 1480 kBq m^{-3} . This deficiency denotes the major importance of knowing all the aspects that affect transport and deposition of radionuclides. It is unexpected what would have happened if the official authorities of ex-USSR evacuated an area of several thousand inhabitants by mistake.

However, the measurements carried out by several accredited laboratories throughout Europe showed that there was transport to many other countries (Fig. 14). A more reliable deposition of ^{137}Cs is reflected by the second run of the model, where ^{137}Cs in the real emission altitude was injected (RG19L). The results are shown in Fig. 15. The transport as well as the dry deposition of ^{137}Cs occurred also throughout Northern European countries especially in the first months after the accident. In addition, the observed precipitation resulted in deposition of higher amounts of ^{137}Cs in specific areas of Sweden and Finland. However, a comparison of the total cumulative deposition of ^{137}Cs simulated by the model to the observed one (De Cort et al., 1998, Fig. 14) showed that the levels of ^{137}Cs deposition are overestimated over Central Europe. The Atlas indicates total deposition inventories of less than 10 kBq m^{-2} , whereas the total deposition inventories estimated in the model were found between 10 and 40 kBq m^{-2} .

The depositional patterns of RG39L simulation of the Chernobyl accident (Fig. 16) are different. The model is not able to estimate the radioactive contamination in the northern countries (in Finland and Sweden), although enhanced depositions were estimated more easterly. Despite these deficiencies the model managed to estimate the increased contamination in the Alpine environment. It has been reported (De Cort et al., 1998) and can be also seen here (Fig. 14) that ^{137}Cs have been deposited in the Alps

after the accident, as a results of the intense precipitation. Moreover, the model also predicted effectively the deposition over North Greece.

As expected, the zoom-version of the model (Fig. 17) provides more discrete results of ^{137}Cs deposition over Europe. The relative distribution of ^{137}Cs deposition is similar to the Atlas, although underestimated, whereas some extremely high values of total cumulative deposition appeared in central Europe. The high deposition observed in Sweden is of the same magnitude and also, at the same location as those presented in Atlas. Another good example is the high total cumulative deposition observed in Russia (north-easterly of the Chernobyl NPP) (Carbol et al., 2003), which is predicted by the model accurately (see also Fig. 14). Finally, in Greece, where enhanced depositions were observed in continental regions (Kritidis et al., 1990; Kritidis and Florou, 1995), and the model predicted them efficiently (see also Fig. 14). Despite the overestimations observed in Central Europe and underestimations in the highly contaminated areas, taking into account the heterogeneity of the direct measurements and the method used to create the Atlas map (inverse distance weighted interpolation method), one could note that the model gives remarkably good results.

5.4 Comparison with depositional observations reported by European countries

Figure 18 shows the location of the measurement stations where measurements of the cumulative total deposition were carried out and presented in the REM-database. Over 4,000 measurements from 20 European countries were used to evaluate and assess the modeling results in terms of the total cumulative deposition of ^{137}Cs . However, no data from Ukraine, Belarus and Russia were available at the EU-JRC. Table 4 shows the respective results of the statistical tests used in order to examine the relevance of the datasets (REM vs RG19L(S), RG19L, RG39L and Z19L, respectively) in contrast to the real-time measurements for ^{137}Cs deposition. The Spearman correlation coefficient was estimated to range from 0.46 to 0.57 with 95 % confident level, whereas the Kendall's tau (τ) rank correlation coefficient was estimated to vary between 0.33

Simulations of the transport and deposition of ^{137}Cs after Chernobyl

N. Evangelidou et al.

Title Page

Abstract

Introduction

Conclusions

References

Tables

Figures



Back

Close

Full Screen / Esc

Printer-friendly Version

Interactive Discussion



Simulations of the transport and deposition of ^{137}Cs after Chernobyl

N. Evangeliou et al.

Title Page

Abstract

Introduction

Conclusions

References

Tables

Figures

⏪

⏩

◀

▶

Back

Close

Full Screen / Esc

Printer-friendly Version

Interactive Discussion



and 0.42, (with 95 % confident level) (Table 4), which shows the dependence between model datasets and observations. In fact, the results obtained from the different model runs (RG19L, RG39L and Z19L) were also contiguous presenting high coefficients (> 0.7). Moreover, Fig. 19 depicts the Box and Whisker plots for the datasets in terms of the total cumulative deposition of ^{137}Cs . There is an obvious trend of the model to underestimate the deposition of ^{137}Cs in the countries examined taking into consideration the boxes corresponding to 25–75 % of the values, although these ranges were similar. For the comparisons of the model to observations of the deposition of ^{137}Cs , reduced though nevertheless realistic agreement can be claimed, taking into account the inherent uncertainties based on the multitude and the complexity of the simulated removal processes (sedimentation, dry and wet deposition). In most cases there is close coincidence between the modeled and measured deposition inventories of ^{137}Cs , although the simulated deposition fluxes underpredict measured ones by a factor of three in extreme cases. However, the model shows the arrival of high concentrations of radioactively contaminated aerosols at central European countries, and the same transport has been verified by previous models and certified by surface activity concentration measurements.

Figure 20 gives a more detailed view of the comparisons for each of the 20 European countries. It depicts linear regression scatter plots of the total ^{137}Cs deposition based on individual measurements of each country (REM database) in descending order, in terms of the best linear fitting, as well as the respective calculated biases from the comparison with the observations. Given the large heterogeneity of the samples and the 50 % uncertainty of the emissions, the model results are in very good agreement with observations. The best performance was achieved for 14 countries (ex-Yugoslavia, Spain, Hungary, Italy, Finland, Sweden, Greece, UK, Netherlands, Switzerland, Belgium, Germany, Norway and France) with correlation coefficients between 0.4 and 0.9, whereas the estimated average bias was -0.81 ± 0.15 for the RG19L run and the Z19L run and lower for the 39 level run (-0.25 ± 0.91). This seems very convenient if compared with other model assessments, which have showed biases around 1.3 for

Simulations of the transport and deposition of ^{137}Cs after Chernobyl

N. Evangeliou et al.

Title Page

Abstract

Introduction

Conclusions

References

Tables

Figures

⏪

⏩

◀

▶

Back

Close

Full Screen / Esc

Printer-friendly Version

Interactive Discussion

5 a better resolved map similar to Atlas was obtained. However, there is a general trend for underestimation in the deposition, which could be attributed to the prevailing environmental processes and the large uncertainties of the source term, as well as to the background deposition of ^{137}Cs from releases occurred prior to the accident that the model do not account for. The high vertical resolution of 39 levels can be useful only when the exact injection altitude is known. The increased number of levels in the boundary layer resulted in a different dispersion and deposition of ^{137}Cs . When a moderate vertical resolution was used (19 layers in the RG19L run) the results were better. The accurate knowledge of the height of the emission is crucial in order to obtain credible transport and deposition of ^{137}Cs . The resulting transport and deposition, when surface emissions were assumed, appeared to be local event in comparison to what really happened after the accident.

10 In all realistic situations studied (presenting the real injection altitude) an ecological half-life of 6–9 days was estimated for the global atmospheric burden of ^{137}Cs . In fact, previous modeling studies give global average half-lives of aerosols in the atmosphere on the order of 3–7 days, whereas for the Chernobyl and the recent Fukushima NPP accident a maximum of 10 days has been reported.

15 In addition, the arrival times of ^{137}Cs in the model in comparison with the observations showed satisfactory correlations (0.46–0.65). Expected lack of dependence was estimated when surface emissions were assumed. The model is able to simulate and predict the development of the specific activity fields with high efficiency, although rarely underestimated. This is expected taking into account the uncertainties of the source term, the deposition processes and the heterogeneity in the samples. However, statistical tests applied to the respective datasets proved a likely dependence.

20 A general conclusion is that the high resolved grid gives results that track closely the observations, especially in the first days of the emissions. This imposes the essential usage of modeling applications as tools for the decision makers, given that the first days of a nuclear accident are very important for life, in terms of addressing the appropriate evacuation criteria for the radiation protection of the population.

Simulations of the transport and deposition of ^{137}Cs after Chernobyl

N. Evangeliou et al.

Title Page

Abstract

Introduction

Conclusions

References

Tables

Figures

⏪

⏩

◀

▶

Back

Close

Full Screen / Esc

Printer-friendly Version

Interactive Discussion



There is a critical need for open data policy after accidental releases. It is a pity that no data from all European countries are present in the public section of the REM database. The paper shows the importance of knowing the emission height of the source in such studies and how much it affects the dispersion and deposition of ^{137}Cs . However, only speculations can be made about the real altitude where ^{137}Cs was injected in the atmosphere and therefore, an uncertainty of 50 % is always used in the case of Chernobyl. Nowadays, the existence of several modeling tools is able to predict the overall details of the emission after a NPP accident (e.g. using inverse modeling). Knowing the exact core inventory by the official authorities or the real emissions during the first days, these dispersion models are able to predict the fate of the radioactive fallout. It is important that such an effort has been made after the recent accident in Japan where the IAEA has created a website with different databases for the Japanese authorities.

Supplementary material related to this article is available online at:
<http://www.atmos-chem-phys-discuss.net/13/7681/2013/acpd-13-7681-2013-supplement.zip>

Acknowledgements. The authors would like to appreciate the funding source of the project (GIS Climat-Environnement-Société, <http://www.gisclimat.fr/projet/radioclimfire>). This work was granted access to the HPC resources of [CCRT/TGCC/CINES/IDRIS] under the allocation 2012-t2012012201 made by GENCI (Grand Equipement National de Calcul Intensif). Acknowledgements are also owed to Mr. Patrick Brockman who initiated us in the secrets of Ferret Analysis Scripting Toolbox and to the National Oceanic and Atmospheric Administration – Pacific Marine Environmental Laboratory (NOAA–PMEL) which created and shared the tool in public. The authors would like to acknowledge the Alfred Wegener Institute for Polar and Marine Research (AWI) and the Unidata community, as well, for releasing in public the free software Ocean Data View (ODV) and Integrated Data Viewer (IDV), respectively.

The publication of this article is financed by CNRS-INSU.

References

- Albergel, A., Martin, D., Strauss, B., and Gros, J.-M.: The Chernobyl accident: modeling of dispersion over Europe of the radioactive plume and comparison with air activity measurements, *Atmos. Environ.*, 22, 2431–2444, 1988.
- ApSimon H. M., Goddard A. J. H., and Wrigley J.: Long-range atmospheric dispersion of radioisotopes, the MESOS model, *Atmos. Environ.*, 19, 113–125, 1985.
- ApSimon H. M., Wilson J. J. N., and Scott P. A.: Assessment of the Chernobyl release in the immediate aftermath of the accident, *Nucl. Energy*, 26, 295–301, 1987.
- Balkanski, Y. J., Jacob, D. J. Arimoto, R., and Kritz, M. A.: Distribution of ^{222}Rn over the North Pacific: implications for continental influences, *J. Atmos. Chem.*, 14, 353–371, 1992.
- Balkanski, Y. J., Jacob, D. J., Gardner, G. M., and G. K. K. Turekian: transport and residence times of tropospheric aerosols inferred from a global three-dimensional simulation of ^{210}Pb , *J. Geophys. Res.*, 98, 20573–20586, 1993.
- Ballestra, S. B., Holm, E., Walton, A., and Whitehead, N. E.: Fallout deposition at Monaco following the Chernobyl accident, *J. Environ. Radioact.*, 5, 391–400, 1987.
- Bonelli, P., Calori, G., and Finzi, G.: A fast long-range transport model for operational use in episode simulation, application to the Chernobyl accident, *Atmos. Environ.*, 26, 2523–2535, 1992.
- Brandt, J., Christensen, J. H., and Frohn, L. M.: Modelling transport and deposition of caesium and iodine from the Chernobyl accident using the DREAM model, *Atmos. Chem. Phys.*, 2, 397–417, doi:10.5194/acp-2-397-2002, 2002.

Simulations of the transport and deposition of ^{137}Cs after Chernobyl

N. Evangelidou et al.

Title Page

Abstract

Introduction

Conclusions

References

Tables

Figures

⏪

⏩

◀

▶

Back

Close

Full Screen / Esc

Printer-friendly Version

Interactive Discussion

Simulations of the transport and deposition of ¹³⁷Cs after Chernobyl

N. Evangeliou et al.

Title Page

Abstract

Introduction

Conclusions

References

Tables

Figures

⏪

⏩

◀

▶

Back

Close

Full Screen / Esc

Printer-friendly Version

Interactive Discussion

Contract Administration Branch, P-902, Washington DC 20555, Technical report, 121 pp., 1991.

Hass, H., Memmesheimer, M., Geiss, H., Jakobs, H. J., Laube, M., and Ebel, A.: Simulation of the Chernobyl radioactive cloud over Europe using EURAD model, *Atmos. Environ.*, 24, 673–692, 1990.

Hatano, Y., Hatano, N., Amano, H., Ueno, T., Sukhoruchkin, A. K., and Kazakov, S. V.: Aerosol migration near Chernobyl: long-term data and modeling, *Atmos. Environ.*, 32, 2587–2594, 1998.

Hauglustaine, D. A., Hourdin, F., Walters, S., Jourdain, L., Filiberti, M.-A., Larmarque, J.-F., and Holland, E. A.: Interactive chemistry in the Laboratoire de Météorologie Dynamique general circulation model: description and background tropospheric chemistry evaluation. *J. Geophys. Res.*, 109, D04314, doi:10.1029/2003JD003957, 2004.

Hourdin, F., and Issartel, J. P.: Sub-surface nuclear tests monitoring through the CTBT xenon network, *Geophys. Res. Lett.*, 27, 2245–2248, 2000.

Huneus, N., Schulz, M., Balkanski, Y., Griesfeller, J., Prospero, J., Kinne, S., Bauer, S., Boucher, O., Chin, M., Dentener, F., Diehl, T., Easter, R., Fillmore, D., Ghan, S., Ginoux, P., Grini, A., Horowitz, L., Koch, D., Krol, M. C., Landing, W., Liu, X., Mahowald, N., Miller, R., Morcrette, J.-J., Myhre, G., Penner, J., Perlwitz, J., Stier, P., Takemura, T., and Zender, C. S.: Global dust model intercomparison in AeroCom phase I, *Atmos. Chem. Phys.*, 11, 7781–7816, doi:10.5194/acp-11-7781-2011, 2011.

Hwang, W. T., Kim, E. H., Suh, K. S., Jeong, H. J., Han, M. H., and Lee, C. W.: Influence of predictive contamination to agricultural products due to dry and wet processes during an accidental release of radionuclides, *Ann. Nucl. Energy*, 30, 1457–1471, 2003.

International Atomic Energy Agency (IAEA): Regulations for the Safe Transport of Radioactive Material, IAEA Safety Requirements, no. TS-R-1, Vienna, 2005.

International Atomic Energy Agency (IAEA): Environmental consequences of the Chernobyl accident and their remediation: twenty years of experience, Report of the Chernobyl Forum Expert Group ‘Environment’, Radiological Assessment Reports Series, Vienna, 2006.

International Atomic Energy Agency (IAEA): Regulations for the Safe Transport of Radioactive Material, IAEA Safety Requirements, no. TS-R-1, Vienna, 2009.

Ishikawa, H.: Evaluation of the effect of horizontal diffusion on the long-range atmospheric transport simulation with Chernobyl data, *J. Appl. Meteorol.*, 34, 1653–1665, 1995.

Simulations of the transport and deposition of ^{137}Cs after Chernobyl

N. Evangeliou et al.

Title Page

Abstract

Introduction

Conclusions

References

Tables

Figures

⏪

⏩

◀

▶

Back

Close

Full Screen / Esc

Printer-friendly Version

Interactive Discussion

- Jacob, D. J., Prather, M. J., Wofsy, S. C., and McElroy, M. B.: Atmospheric distribution of ^{85}Kr simulated with a general circulation model JGR, *J. Geophys. Res.*, 92, 6614–6626, 1987.
- Jacob, D. J., Prather, M. J., Rasch, P. J., Shia, R. L., Balkanski, Y. J., Beagley, S. R., Bergmann, D. J., Blackshear, W. T., Brown, M., Chiba, M., Chipperfield, M. P., De Grandpré, J., Dignon, J. E., Feichter, J., Genthon, C., Grose, W. L., Kasibhatla, P. S., Köhler, I., Kritz, M. A., Law, K., Penner, J. E., Ramonet, M., Reeves, C. E., Rotman, D. A., Stockwell, D. Z., Van Velthoven, P. F. J., Verver, G., Wild, O., Yang, H., and Zimmermann, P.: Evaluation and intercomparison of global atmospheric transport models using ^{222}Rn and other short-lived tracers, *J. Geophys. Res.*, 102, 5953–5970, 1997.
- Klug, W., Graziani, G., Grippa, G., Pierce, D., and Tassone, C.: Evaluation of Long Range Atmospheric Transport Models Using Environmental Radioactivity Data from the Chernobyl Accident, The ATMES Report, Elsevier Applied Science, London and New York, 366 pp., 1992.
- Koch, D., Schulz, M., Kinne, S., McNaughton, C., Spackman, J. R., Balkanski, Y., Bauer, S., Berntsen, T., Bond, T. C., Boucher, O., Chin, M., Clarke, A., De Luca, N., Dentener, F., Diehl, T., Dubovik, O., Easter, R., Fahey, D. W., Feichter, J., Fillmore, D., Freitag, S., Ghan, S., Ginoux, P., Gong, S., Horowitz, L., Iversen, T., Kirkevåg, A., Klimont, Z., Kondo, Y., Krol, M., Liu, X., Miller, R., Montanaro, V., Moteki, N., Myhre, G., Penner, J. E., Perlwitz, J., Pitari, G., Reddy, S., Sahu, L., Sakamoto, H., Schuster, G., Schwarz, J. P., Seland, Ø., Stier, P., Takegawa, N., Takemura, T., Textor, C., van Aardenne, J. A., and Zhao, Y.: Evaluation of black carbon estimations in global aerosol models, *Atmos. Chem. Phys.*, 9, 9001–9026, doi:10.5194/acp-9-9001-2009, 2009.
- Kornberg, H. A.: The use of element-pairs in radiation hazard assessment, *Health Phys.*, 6, 46–62, 1961.
- Kristiansen, N. I., Stohl, A., and Wotawa, G.: Atmospheric removal times of the aerosol-bound radionuclides ^{137}Cs and ^{131}I measured after the Fukushima Dai-ichi nuclear accident – a constraint for air quality and climate models, *Atmos. Chem. Phys.*, 12, 10759–10769, doi:10.5194/acp-12-10759-2012, 2012.
- Kritidis, P.: Radioactive contamination of the environment, in: *Ourselves and Radioactivity*, edited by: Verganelakis, A., Kritidis, P., Economou, L., Papazoglou, I., Papanikolaou, E., Sideris, L., and Simopoulos, T., University of Crete Publications, Heraklion, Greece, 235–270, 1989 (in Greek).

Simulations of the transport and deposition of ^{137}Cs after Chernobyl

N. Evangelidou et al.

Title Page

Abstract

Introduction

Conclusions

References

Tables

Figures

⏪

⏩

◀

▶

Back

Close

Full Screen / Esc

Printer-friendly Version

Interactive Discussion

- Kritidis, P. and Florou, H.: Environmental study of radioactive caesium in Greek lake fish after the Chernobyl accident, *J. Environ. Radioact.*, 28, 285–293, 1995.
- Kritidis, P., Florou, H., and Papanicolaou, E.: Delayed and late impact of the Chernobyl accident on the Greek environment, *Radiat. Prot. Dosim.*, 30, 187–190, 1990.
- 5 Lange, R., Dickerson, M. H., and Gudiksen, P. H.: Dose estimates from the Chernobyl accident, *Nucl. Technol.*, 82, 311–323, 1988.
- Lee, D. S., Nemitz, E., Fowler, D., and Kingdon, R. D.: Modelling atmospheric mercury transport and deposition across Europe and the UK, *Atmos. Environ.*, 35, 5455–5466, 2001.
- Lelieveld, J., Kunkel, D., and Lawrence, M. G.: Global risk of radioactive fallout after major
10 nuclear reactor accidents, *Atmos. Chem. Phys.*, 12, 4245–4258, doi:10.5194/acp-12-4245-2012, 2012.
- Liu, H., Jacob, D. J., Bey, I., and Yantosca, R. M.: Constraints from ^{210}Pb and ^7Be on wet deposition and transport in a global three-dimensional chemical transport model driven by assimilated meteorological fields, *J. Geophys. Res.*, 106, 12109–12128, 2001.
- 15 Mari, C., Jacob, D. J., and Bechtold, P.: Transport and scavenging of soluble gases in a deep convective cloud, *J. Geophys. Res.*, 105, 22255–22268, 2000.
- Mattsson, S. and Vesanen, R.: Patterns of Chernobyl fallout in relation to local weather conditions, *Environ. Int.*, 14, 177–180, 1988.
- Morino, Y., Ohara, T., and Nishizawa, M.: Atmospheric behavior, deposition, and budget of radioactive materials from the Fukushima Daiichi nuclear power plant in March 2011, *Geophys. Res. Lett.*, 38, L00G11, doi:10.1029/2011GL048689, 2011.
- 20 Olivé, D. J. L., Cariolle, D., Teyssère, H., Salas, D., Voldoire, A., Clark, H., Saint-Martin, D., Michou, M., Karcher, F., Balkanski, Y., Gauss, M., Dessens, O., Koffi, B., and Sausen, R.: Modeling the climate impact of road transport, maritime shipping and aviation over the period 1860–2100 with an AOGCM, *Atmos. Chem. Phys.*, 12, 1449–1480, doi:10.5194/acp-12-1449-2012, 2012.
- 25 Peplow, M.: Counting the dead (special report about the death toll of the Chernobyl accident), *Nature*, 440, 982–983, 2006.
- Piedelievre, J. P., Musson-Genon, L., and Bompay, F.: MEDIA – an Eulerian model for atmospheric dispersion: first validation on the Chernobyl release, *J. Appl. Meteorol.*, 29, 1205–1220, 1990.
- 30

Simulations of the transport and deposition of ¹³⁷Cs after Chernobyl

N. Evangeliou et al.

Title Page

Abstract

Introduction

Conclusions

References

Tables

Figures

⏪

⏩

◀

▶

Back

Close

Full Screen / Esc

Printer-friendly Version

Interactive Discussion

- Potiriadis, C., Kolovou, M., Clouvas, A., and Xanthos, S.: Environmental radioactivity measurements in Greece following the Fukushima Daichi nuclear accident, *Radiat. Prot. Dosim.*, 150, 441–447 doi:10.1093/rpd/ncr423, 2011.
- Prather, M., McElroy, M., Wofsy, S., Russell, G., Rind, D.: Chemistry of the global troposphere: fluorocarbons as tracers of air motion, *J. Geophys. Res.*, 92, 6579–6613, 1987.
- Ritchie, J. C., and McHenry, J. R.: Application of radioactive fallout cesium-137 for measuring soil erosion and sediment accumulation rates and patterns: a review, *J. Environ. Qual.*, 19, 215–233, 1990.
- Salvadori, G., Ratti, S. P., and Belli, G.: Modelling the Chernobyl radioactive fallout (II): a multifractal approach in some European countries, *Chemosphere*, 33, 2359–2371, 1996.
- Seinfeld, J. H. and Pandis S. N.: *Atmospheric Chemistry and Physics*, John Wiley, New York, 1998.
- Sportisse, B.: A review of parameterizations for modelling dry deposition and scavenging of radionuclides, *Atmos. Environ.*, 41, 2683–2698, 2007.
- Stier, P., Feichter, J., Kinne, S., Kloster, S., Vignati, E., Wilson, J., Ganzeveld, L., Tegen, I., Werner, M., Balkanski, Y., Schulz, M., Boucher, O., Minikin, A., and Petzold, A.: The aerosol-climate model ECHAM5-HAM, *Atmos. Chem. Phys.*, 5, 1125–1156, doi:10.5194/acp-5-1125-2005, 2005.
- Szopa, S., Balkanski, Y., Cozic, A., Deandreis, C., Dufresne, J.-L., Hauglustaine, D., Lathiere, J., Schulz, M., Vuolo, R., Yan, N., Marchand, M., Bekki, S., Cugnet, D., Idelkadi, A., Denvil, S., Foujols, M.-A., Caubel, A., and Fortems-Cheiney, A.: Aerosol and ozone changes as forcing for climate evolution between 1850 and 2100, *Clim. Dynam.*, doi:10.1007/s00382-012-1408-y, 2012.
- Valkama, I. and Pollanen, R.: Transport of radioactive materials in convective clouds, in: *Proceedings of the 14th International Conference on Nucleation and Atmospheric Aerosols*, Helsinki, 26–30 August 1996, edited by: Kulmala, M. and Wagner, P. E., 4 pp., 1996.
- Valkama, I., Salonoja, M., Toivonen, H., Lahtinen, J., and Pollanen, R.: Transport of radioactive gases and particles in the Chernobyl accident: comparison of environmental measurements and dispersion calculations, *International Atomic Energy Agency, International Symposium on Environmental Impact of Radioactive Releases*, Vienna, Austria, 8–12 May 1995, IAEA-SM-339/69, 10 pp., 1995.
- Waight, P., Métivier, H., Jacob, P., Souchkevitch, G., Viktorsson, C., Bennett, B., Hance, R., Kumazawa, S., Kusumi, S., Bouville, A., Sinnaeve, J., Ilari, O., and Lazo, E.: Chernobyl Ten

Simulations of the transport and deposition of ^{137}Cs after Chernobyl

N. Evangeliou et al.

Title Page

Abstract

Introduction

Conclusions

References

Tables

Figures

⏪

⏩

◀

▶

Back

Close

Full Screen / Esc

Printer-friendly Version

Interactive Discussion

Years On Radiological and Health Impact, An Assessment by the NEA Committee on 10 Radiation Protection and Public Health, November 1995, OECD Nuclear Agency, available at: <http://www.nea.fr/> (last access: 29 October 2012), 74 pp., 1995.

5 Walcek, C. J., Brost, R. A., Chang, J. S., and Wesely, M. L.: SO_2 , sulfate and HNO_3 deposition velocities computed using regional landuse and meteorological data, Atmos. Environ., 20, 949–964, 1986.

Wesely, M. L.: Parametrization of surface resistances to gaseous dry deposition in regional-scale numerical models, Atmos. Environ., 23, 1293–1304, 1989.

10 Woodhead, D. S.: Levels of radioactivity in the marine environment and the dose commitment to the marine organisms, IAEA–S.M. 158/31, Vienna, 1973.

Yoschenko, V. I., Kashparov, V. A., Protsak, V. P., Lundin, S. M., Levchuk, S. E., Kadygrib, A. M., Zvarich, S. I., Khomutinin, Yu. V., Maloshtan, I. M., Lanshin, V. P., Kovtun, M. V., Tschiersch, J.: Resuspension and redistribution of radionuclides during grassland and forest fires in the Chernobyl exclusion zone: Part I. Fire experiments, J. Environ. Radioact., 86, 143–163, 2006.

Simulations of the transport and deposition of ^{137}Cs after Chernobyl

N. Evangeliou et al.

Title Page

Abstract

Introduction

Conclusions

References

Tables

Figures

◀

▶

◀

▶

Back

Close

Full Screen / Esc

Printer-friendly Version

Interactive Discussion

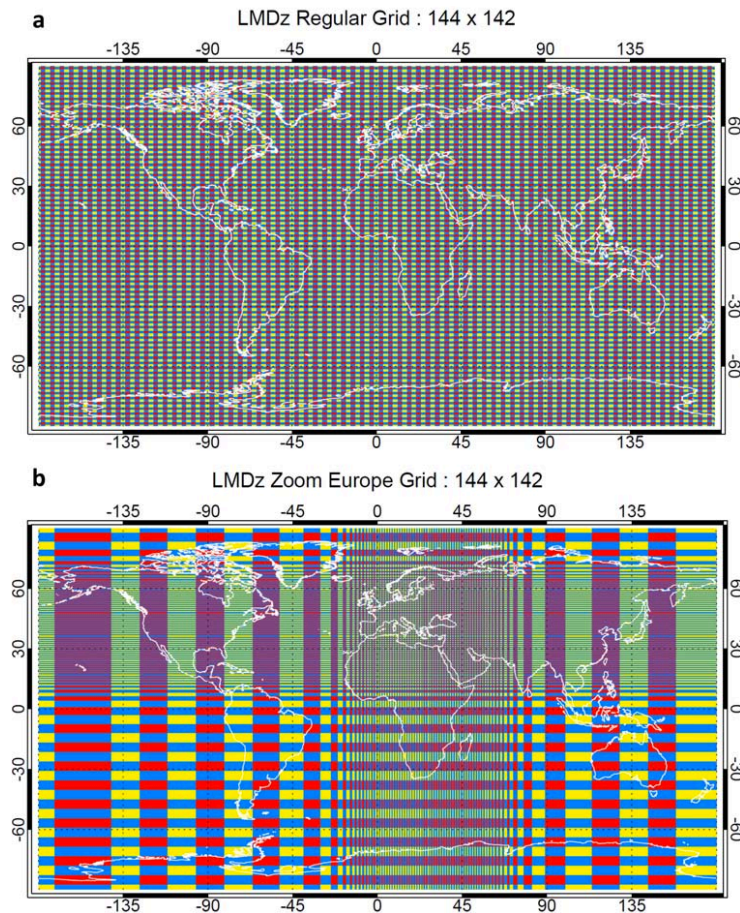


Fig. 1. (a) 144×142 regular grid of the GCM used for the simulations of the Chernobyl accident, (b) 144×142 grid “stretched” over Europe (zoom-version) used for the simulations of the Chernobyl accident using 19 and 39 sigma-p vertical layers.

Simulations of the transport and deposition of ^{137}Cs after Chernobyl

N. Evangeliou et al.

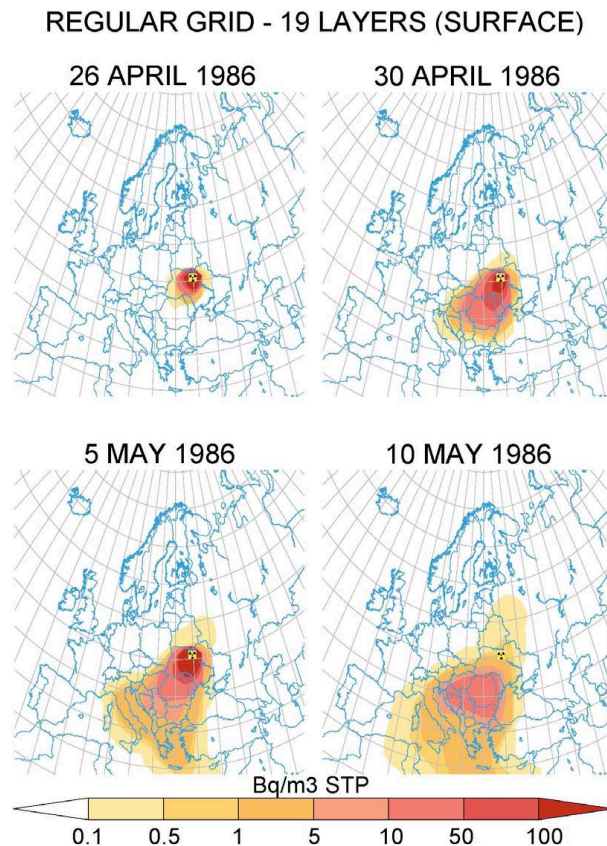


Fig. 2. Daily mean surface ^{137}Cs activity concentrations (in Bq m^{-3} STP) from the Chernobyl accident. Model with regular grid and 19 vertical levels assuming surface emissions (RG19L(S)). The figures show the situation during the first day (26 April 1986), at the end of April (30 April 1986), the last day of the emissions (5 May 1986) and every 10 days until the end of May 1986 (10, 20 and 31 May 1986).

[Title Page](#)[Abstract](#)[Introduction](#)[Conclusions](#)[References](#)[Tables](#)[Figures](#)[◀](#)[▶](#)[◀](#)[▶](#)[Back](#)[Close](#)[Full Screen / Esc](#)[Printer-friendly Version](#)[Interactive Discussion](#)

Simulations of the transport and deposition of ^{137}Cs after Chernobyl

N. Evangeliou et al.

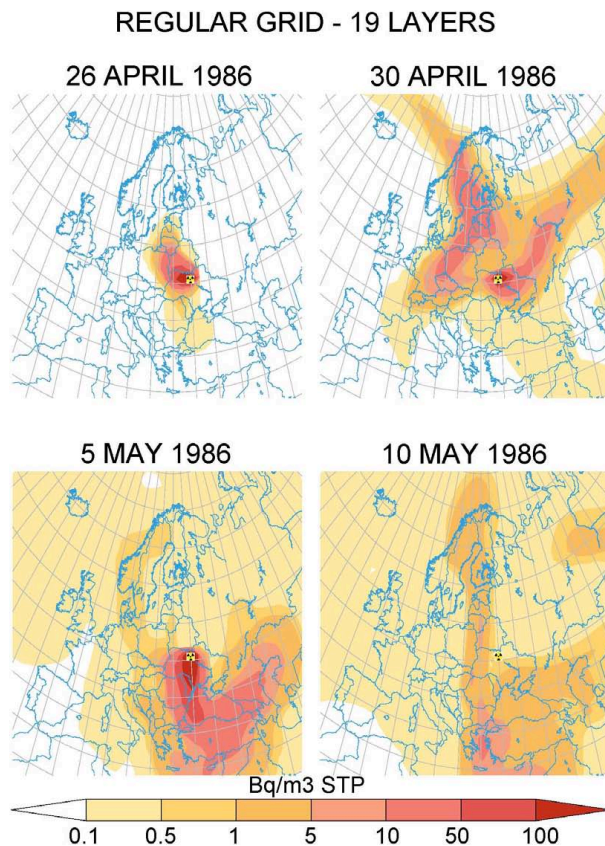


Fig. 3. Daily mean surface ^{137}Cs activity concentrations (in Bq m^{-3} STP) from the Chernobyl accident. Model with regular grid and 19 vertical levels and injection at the real emission height (Table 1) (RG19L). The figures show the situation during the first day (26 April 1986), at the end of April (30 April 1986), the last day of the emissions (5 May 1986) and every 10 days until the end of May 1986 (10, 20 and 31 May 1986).

[Title Page](#)[Abstract](#)[Introduction](#)[Conclusions](#)[References](#)[Tables](#)[Figures](#)[⏪](#)[⏩](#)[⏴](#)[⏵](#)[Back](#)[Close](#)[Full Screen / Esc](#)[Printer-friendly Version](#)[Interactive Discussion](#)

REGULAR GRID - 39 LAYERS

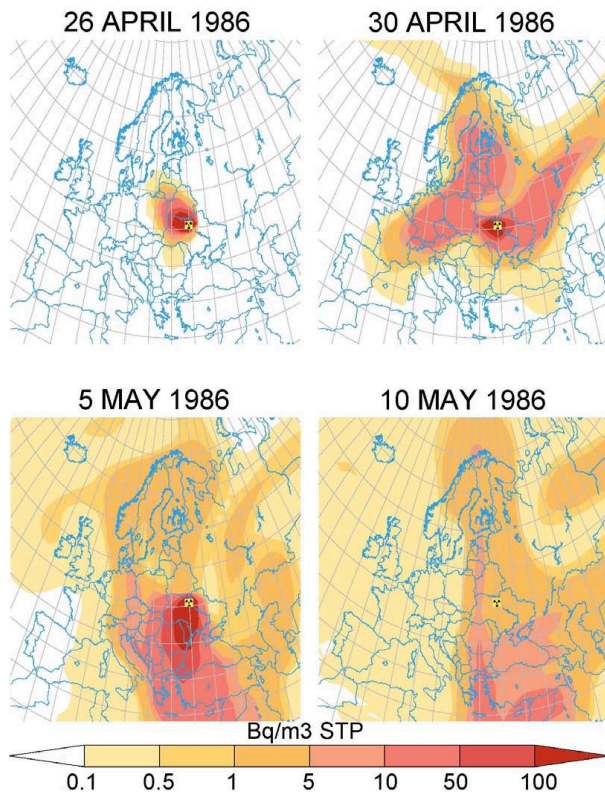


Fig. 4. Daily mean surface ^{137}Cs activity concentrations (in Bq m^{-3} STP) from the Chernobyl accident. Model with regular grid and 39 vertical levels and injection at the real emission height (Table 1) (RG39L). The figures show the situation during the first day (26 April 1986), at the end of April (30 April 1986), the last day of the emissions (5 May 1986) and every 10 days until the end of May 1986 (10, 20 and 31 May 1986).

Title Page

Abstract

Introduction

Conclusions

References

Tables

Figures

◀

▶

◀

▶

Back

Close

Full Screen / Esc

Printer-friendly Version

Interactive Discussion

ZOOM VERSION - 19 LAYERS

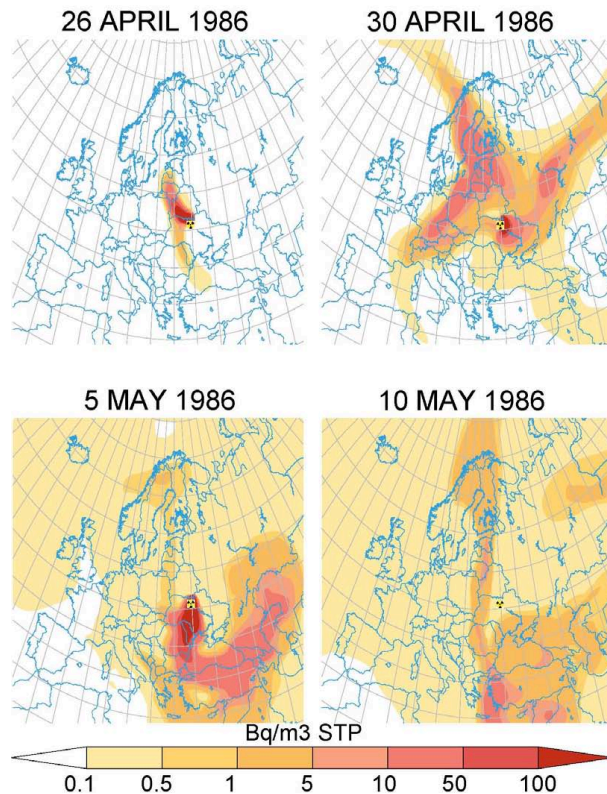


Fig. 5. Daily mean surface ^{137}Cs activity concentrations (in Bq m^{-3} STP) from the Chernobyl accident. Model with regular grid stretched over Europe and 19 vertical levels and injection at the real emission height (Table 1) (Z19L). The figures show the situation during the first day (26 April 1986), at the end of April (30 April 1986), the last day of the emissions (5 May 1986) and every 10 days until the end of May 1986 (10, 20 and 31 May 1986).

Simulations of the transport and deposition of ^{137}Cs after Chernobyl

N. Evangeliou et al.

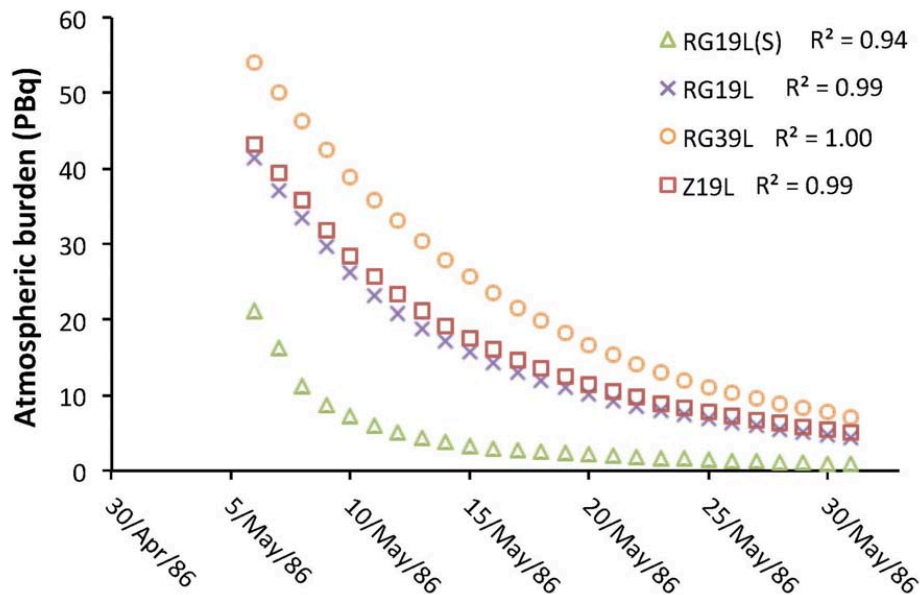


Fig. 6. Exponential decrease of the atmospheric burden of ^{137}Cs (in PBq) for the 4 different simulations of the Chernobyl accident (RG19L(S), RG19L, RG39L and Z19L). This graph was used in order to estimate the ecological half-lives of ^{137}Cs in the atmosphere.

[Title Page](#)
[Abstract](#)
[Introduction](#)
[Conclusions](#)
[References](#)
[Tables](#)
[Figures](#)
[⏪](#)
[⏩](#)
[⏴](#)
[⏵](#)
[Back](#)
[Close](#)
[Full Screen / Esc](#)
[Printer-friendly Version](#)
[Interactive Discussion](#)

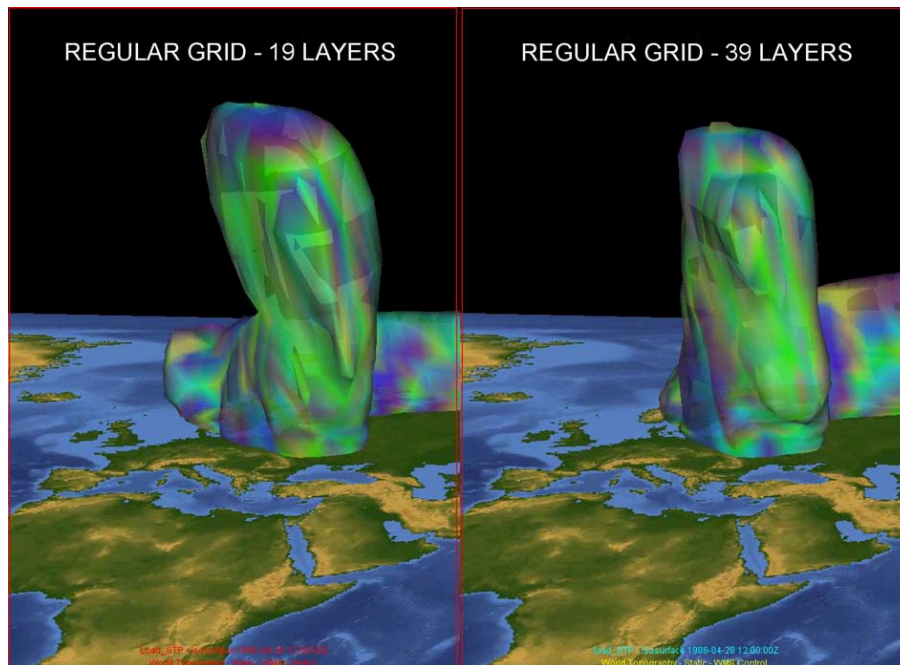


Fig. 7. A three-dimensional mapping of the 0.15 Bq m^{-3} STP iso-surface of ^{137}Cs on the third day after the Chernobyl accident (28 April 12:00 UTC) for 19 (left panel) and 39 vertical levels (right panel). Surface activity concentrations in Bq m^{-3} STP are plotted on the iso-surface with the darker color indicating high concentrations and the lighter lower ones.

Simulations of the transport and deposition of ^{137}Cs after Chernobyl

N. Evangeliou et al.

Title Page	
Abstract	Introduction
Conclusions	References
Tables	Figures
⏪	⏩
◀	▶
Back	Close
Full Screen / Esc	
Printer-friendly Version	
Interactive Discussion	



Simulations of the transport and deposition of ¹³⁷Cs after Chernobyl

N. Evangeliou et al.

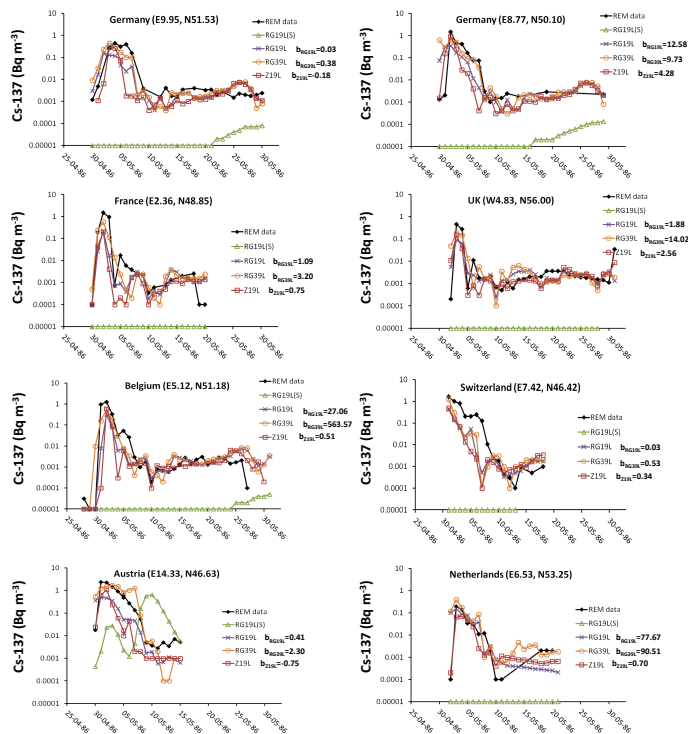


Fig. 8. Comparison of the ¹³⁷Cs surface activity concentrations estimated by all model versions with observations reported in the “REM database” for the Chernobyl accident. The data are available in the website of EU Joint Research Centre in Ispra, Italy (<http://rem.jrc.ec.europa.eu/RemWeb/Index.aspx>). They were examined according to the 3 different directions of the fallout (north, west, south-eastern) on 30 April 1986. Here, the comparison for the countries of central-western Europe is depicted. The estimated biases are also shown for all the runs (b_{RG19L} , b_{RG39L} and b_{Z19L}) except the one where surface emissions assumed.

Title Page

Abstract Introduction

Conclusions References

Tables Figures

◀ ▶

◀ ▶

Back Close

Full Screen / Esc

Printer-friendly Version

Interactive Discussion



Simulations of the transport and deposition of ^{137}Cs after Chernobyl

N. Evangeliou et al.

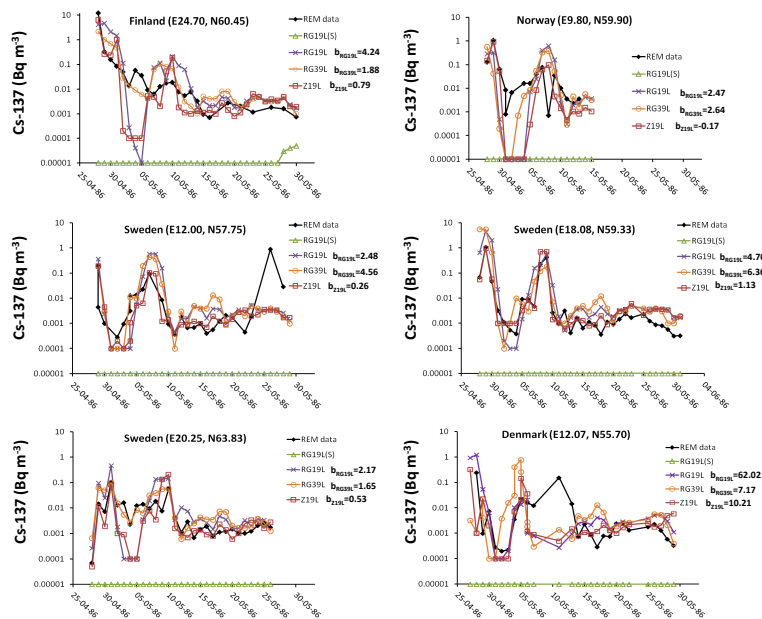


Fig. 9. Comparison of the ^{137}Cs surface activity concentrations estimated by all model versions with observations reported in the “REM database” for the Chernobyl accident. The data are available in the website of EU Joint Research Centre in Ispra, Italy (<http://rem.jrc.ec.europa.eu/RemWeb/Index.aspx>). They were examined according to the 3 different directions of the fallout (north, west, south-eastern) on 30 April 1986. Here, the comparison for the countries of north Europe is depicted. The estimated biases are also shown for all the runs (b_{RG19L} , b_{RG39L} and b_{Z19L}) except for the one where surface emissions assumed.

[Title Page](#)
[Abstract](#)
[Introduction](#)
[Conclusions](#)
[References](#)
[Tables](#)
[Figures](#)
[⏪](#)
[⏩](#)
[⏴](#)
[⏵](#)
[Back](#)
[Close](#)
[Full Screen / Esc](#)
[Printer-friendly Version](#)
[Interactive Discussion](#)

Simulations of the transport and deposition of ^{137}Cs after Chernobyl

N. Evangeliou et al.

Title Page

Abstract

Introduction

Conclusions

References

Tables

Figures



Back

Close

Full Screen / Esc

Printer-friendly Version

Interactive Discussion

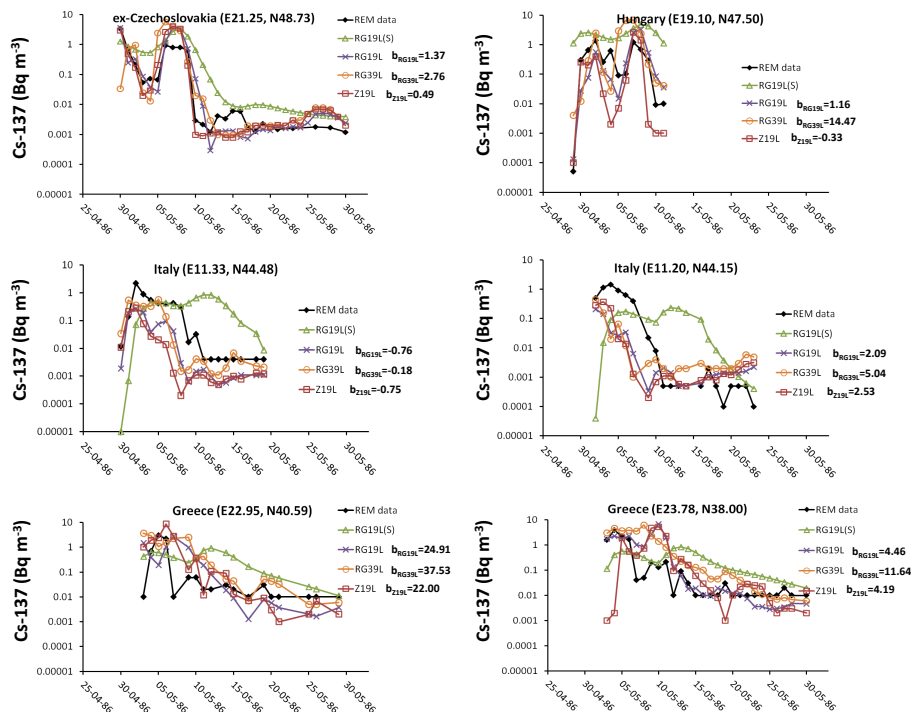


Fig. 10. Comparison of the ^{137}Cs surface activity concentrations estimated by all model versions with observations reported in the “REM database” for the Chernobyl accident. The data are available in the website of EU Joint Research Centre in Ispra, Italy (<http://rem.jrc.ec.europa.eu/RemWeb/Index.aspx>). They were examined according to the 3 different directions of the fallout (north, west, south-eastern) on 30 April 1986. Here, the comparison for the countries of south-eastern Europe is depicted. The estimated biases are also shown for all the runs (b_{RG19L} , b_{RG39L} and b_{Z19L}) except for the one where surface emissions assumed.

Simulations of the transport and deposition of ^{137}Cs after Chernobyl

N. Evangeliou et al.

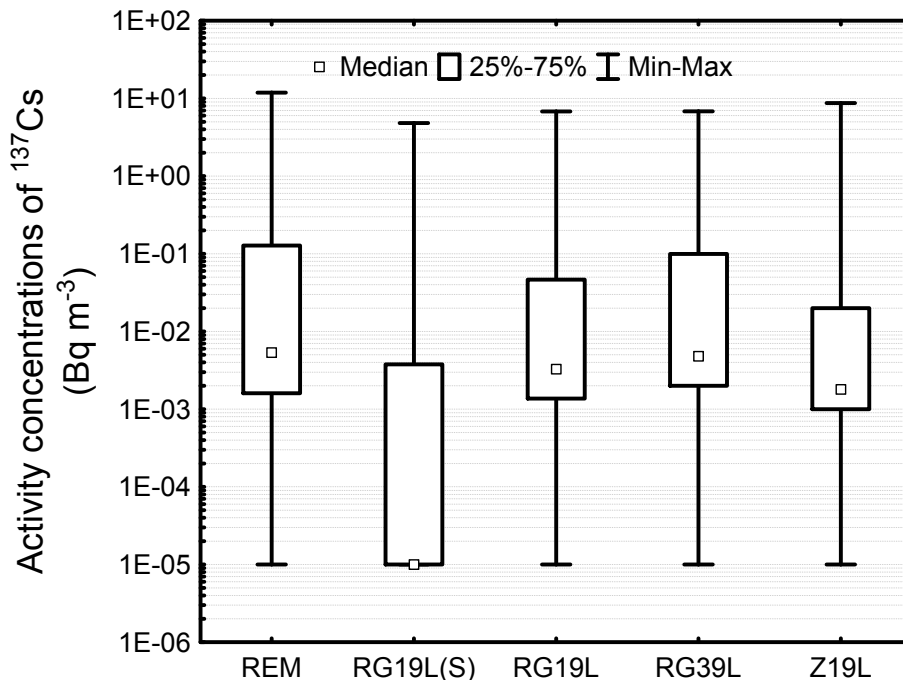


Fig. 11. Box and Whisker plots of the surface activity concentrations of ^{137}Cs obtained from the REM database and from the simulations using all the available versions of the model. The plot depicts the smallest observation (sample minimum), lower quartile, median, upper quartile and the largest observation (sample maximum) ($N = 711$).

Title Page

Abstract

Introduction

Conclusions

References

Tables

Figures

◀

▶

◀

▶

Back

Close

Full Screen / Esc

Printer-friendly Version

Interactive Discussion



Simulations of the transport and deposition of ^{137}Cs after Chernobyl

N. Evangeliou et al.

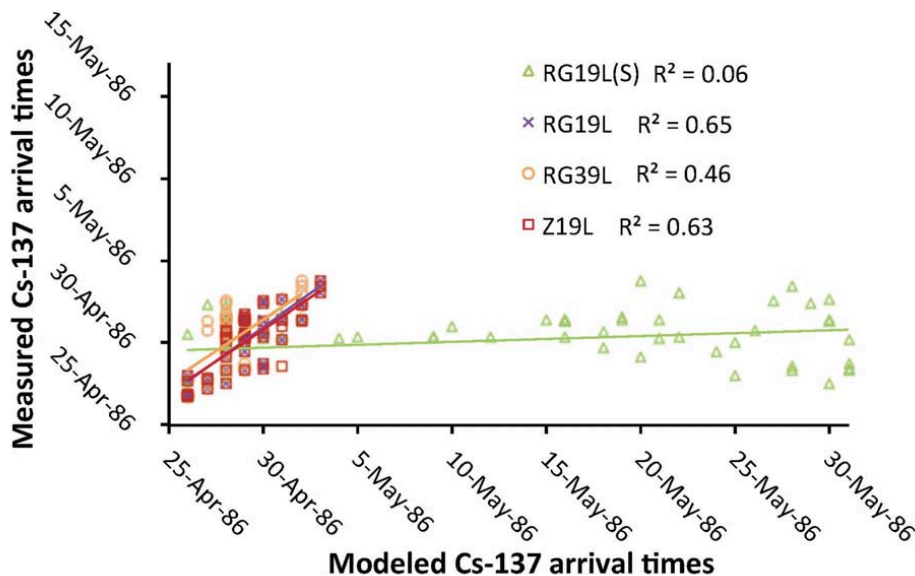


Fig. 12. Estimation of the arrival times of the radioactive fallout of ^{137}Cs after simulation using all model versions (RG19L(S), RG19L, RG39L and Z19L) and comparison with the respective ones obtained from the REM database. The data correspond to time-series measurements from 56 sampling points across Europe.

Title Page

Abstract

Introduction

Conclusions

References

Tables

Figures

⏪

⏩

◀

▶

Back

Close

Full Screen / Esc

Printer-friendly Version

Interactive Discussion



Simulations of the transport and deposition of ^{137}Cs after Chernobyl

N. Evangeliou et al.

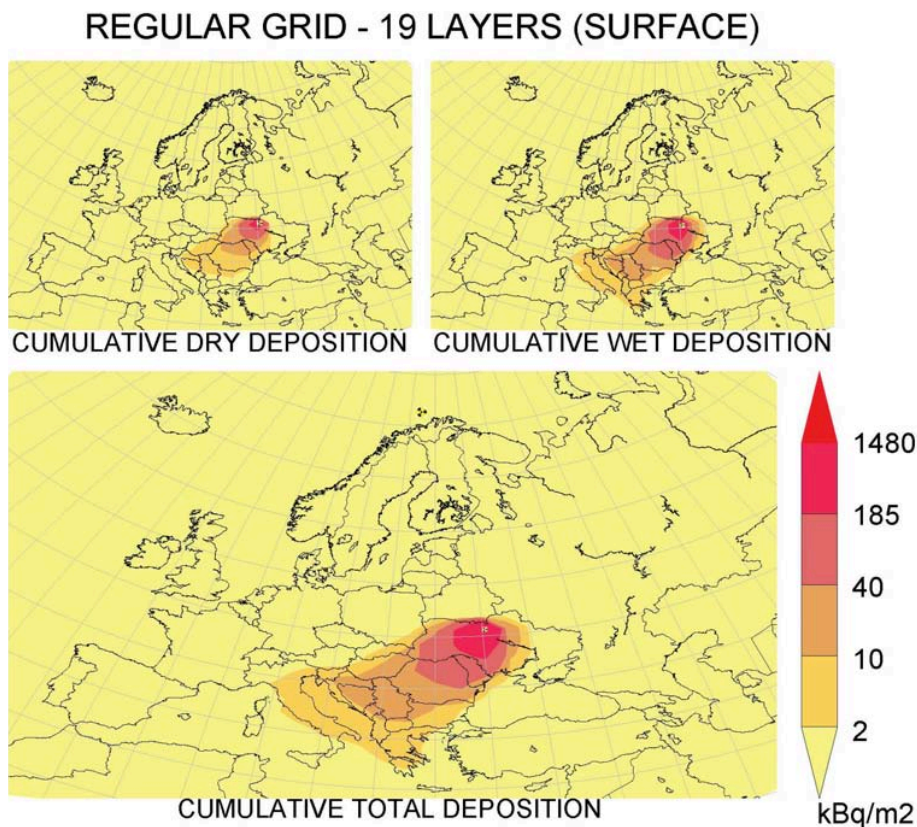


Fig. 13. Cumulative dry, wet and total deposition of ^{137}Cs (kBq m^{-2}) from the day of the accident (26 April 1986) until the end of 1986. Results of the simulation using the regular grid of the model for 19 vertical layers and accounting for source emissions to occur at the surface (RG19L(S)).

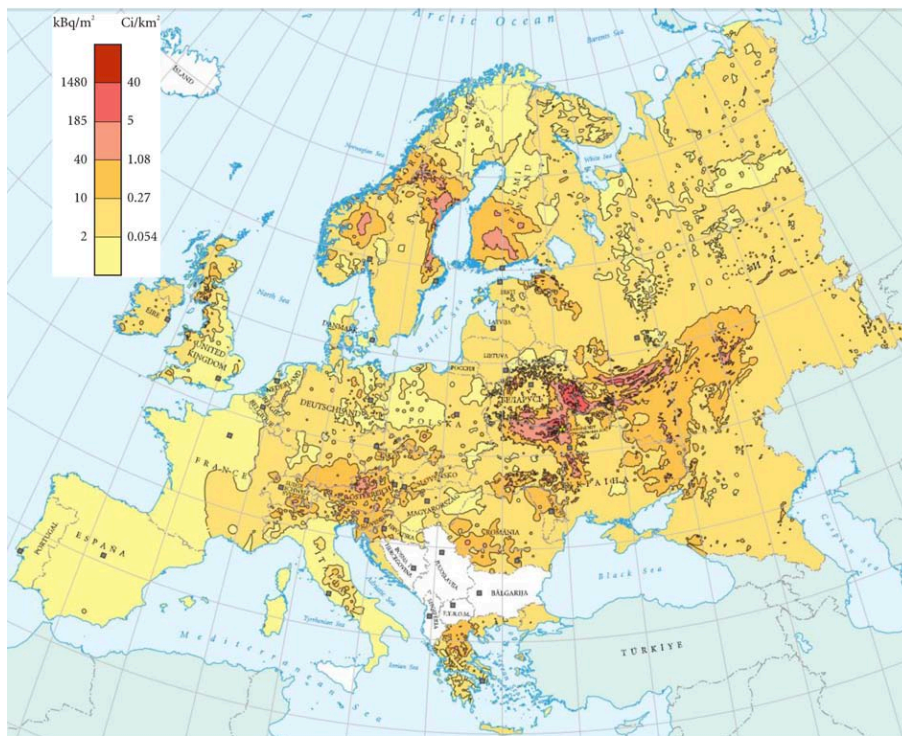


Fig. 14. The Atlas map depicting the total cumulative deposition of ^{137}Cs throughout Europe as a result of the Chernobyl accident and nuclear weapon testing from all available data of the REM database corrected for radioactive decay to 10 May 1986. The map has been published in the “Atlas of caesium deposition on Europe after the Chernobyl accident” (De Cort et al., 1998).

Simulations of the transport and deposition of ^{137}Cs after Chernobyl

N. Evangeliou et al.

Title Page	
Abstract	Introduction
Conclusions	References
Tables	Figures
⏪	⏩
⏴	⏵
Back	Close
Full Screen / Esc	
Printer-friendly Version	
Interactive Discussion	



Simulations of the transport and deposition of ^{137}Cs after Chernobyl

N. Evangeliou et al.

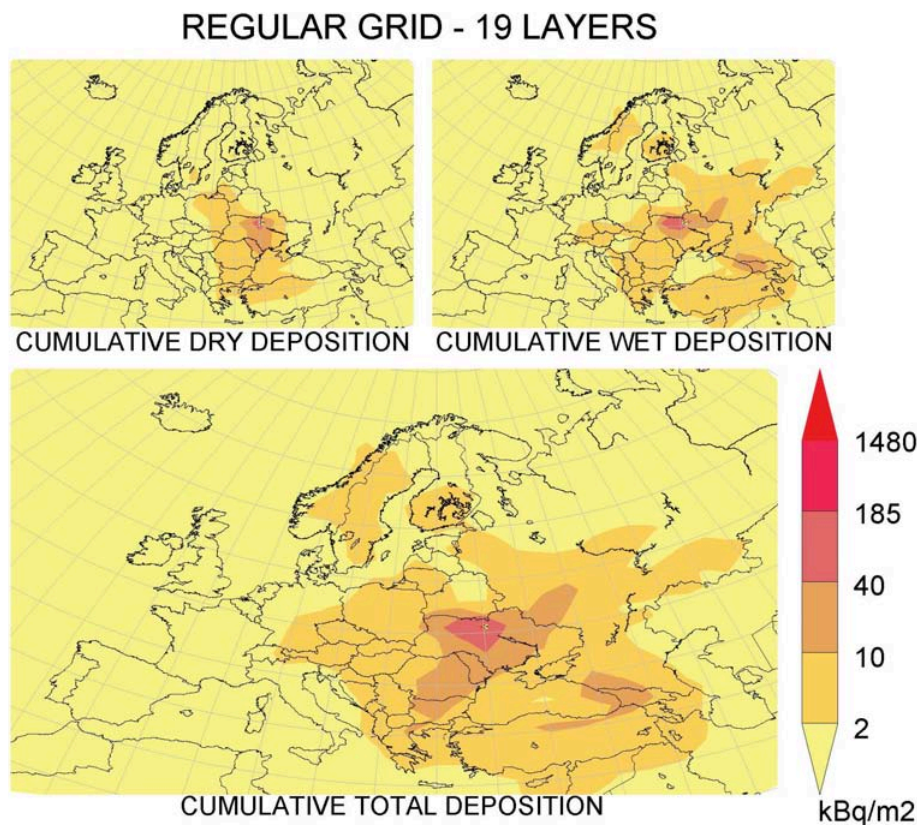


Fig. 15. Cumulative dry, wet and total deposition of ^{137}Cs (kBq m^{-2}) from the day of the accident (26 April 1986) until the end of 1986. Results of the simulation using the regular grid of the model for 19 vertical layers and accounting for the altitude of the emissions with respect to Table 1 (RG19L).

Simulations of the transport and deposition of ^{137}Cs after Chernobyl

N. Evangeliou et al.

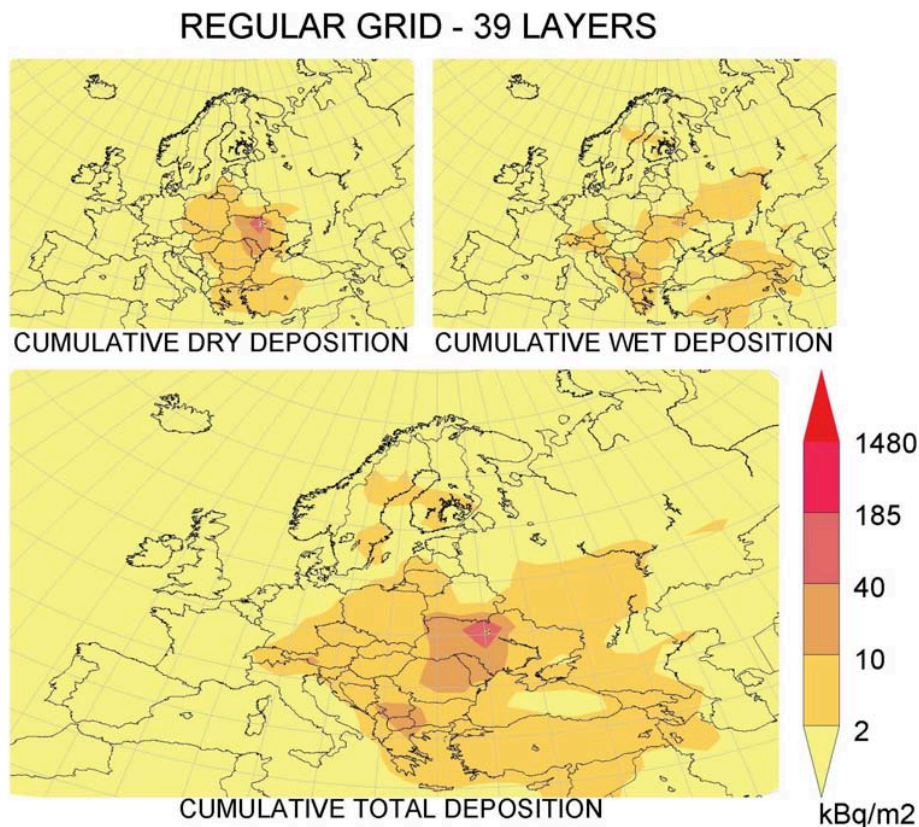


Fig. 16. Cumulative dry, wet and total deposition of ^{137}Cs (kBq m^{-2}) from the day of the accident (26 April 1986) until the end of 1986. Results of the simulation using the regular grid of the model for 39 vertical layers and accounting for the altitude of the emissions with respect to Table 1 (RG39L).

Simulations of the transport and deposition of ^{137}Cs after Chernobyl

N. Evangeliou et al.

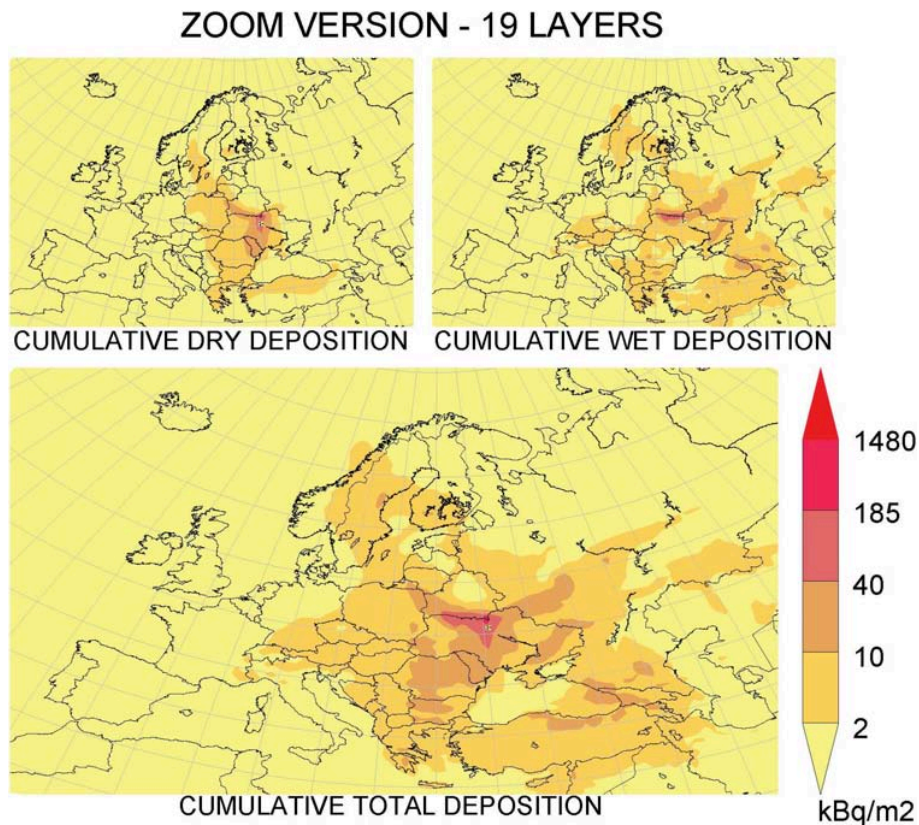


Fig. 17. Cumulative dry, wet and total deposition of ^{137}Cs (kBq m^{-2}) from the day of the accident (26 April 1986) until the end of 1986. Results of the simulation using the zoom-version of the model for 19 vertical layers and accounting for the altitude of the emissions with respect to Table 1.

[Title Page](#)[Abstract](#)[Introduction](#)[Conclusions](#)[References](#)[Tables](#)[Figures](#)[⏪](#)[⏩](#)[⏴](#)[⏵](#)[Back](#)[Close](#)[Full Screen / Esc](#)[Printer-friendly Version](#)[Interactive Discussion](#)

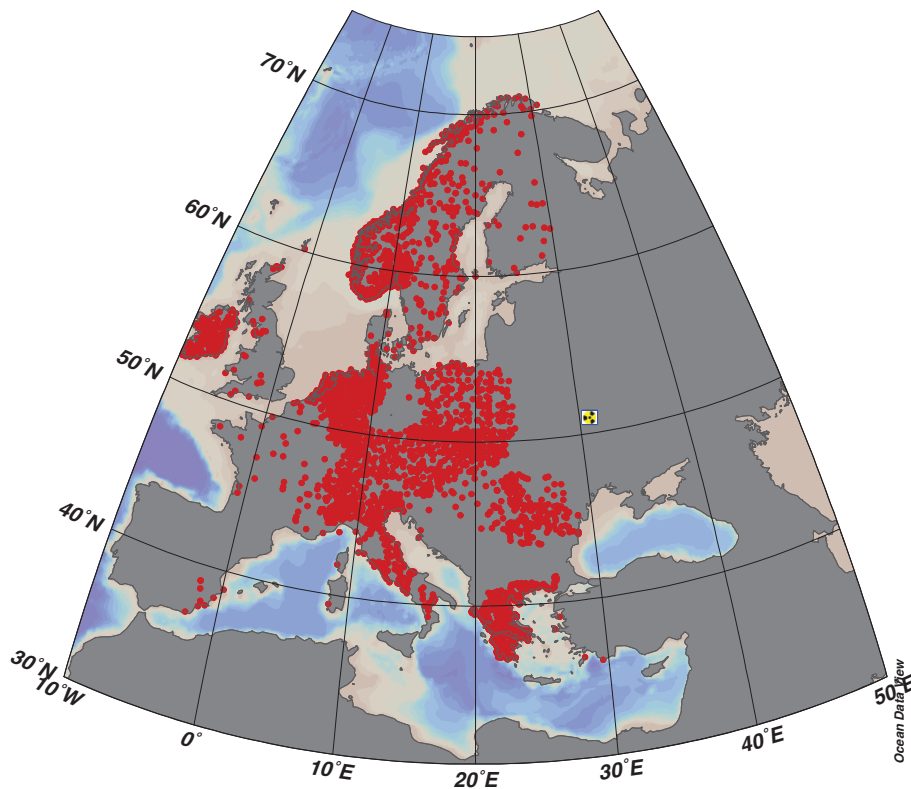


Fig. 18. Location of the sampling stations ($N = 4266$), where measurements of the total deposition of ^{137}Cs after the Chernobyl accident (from the REM database) were carried out. The data were used for the validation of the total deposition of ^{137}Cs resulting from the simulations of the Chernobyl accident using all available versions of the model.

Simulations of the transport and deposition of ^{137}Cs after Chernobyl

N. Evangeliou et al.

Title Page	
Abstract	Introduction
Conclusions	References
Tables	Figures
⏪	⏩
◀	▶
Back	Close
Full Screen / Esc	
Printer-friendly Version	
Interactive Discussion	



Simulations of the transport and deposition of ^{137}Cs after Chernobyl

N. Evangeliou et al.

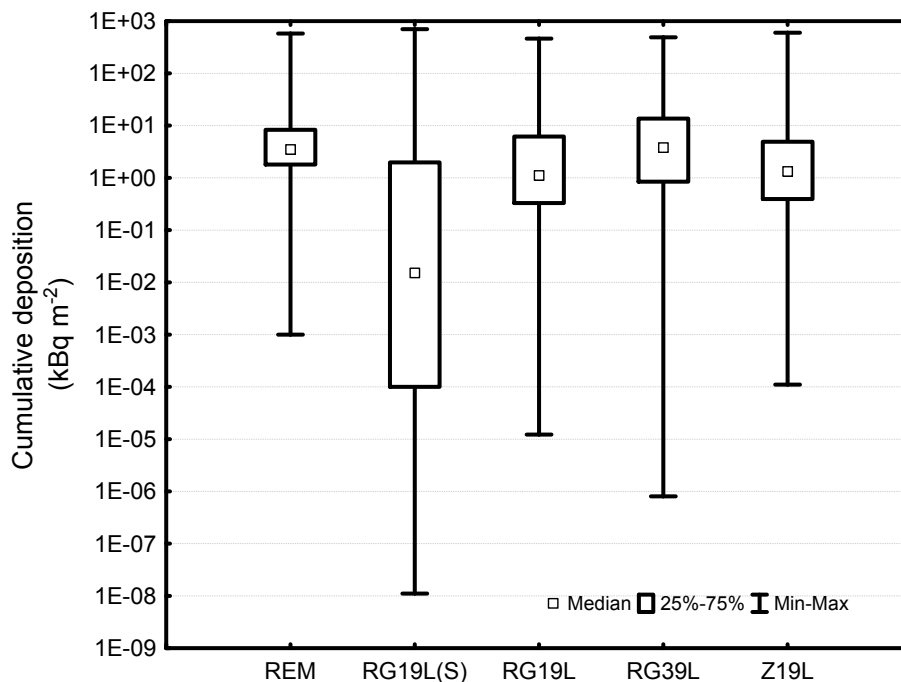


Fig. 19. Box and Whisker plots of the cumulative total deposition of ^{137}Cs obtained from the REM database and from the simulations using all the available versions of the model (RG19L(S), RG19L, RG39L and Z19L). The plot depicts the smallest observation (sample minimum), lower quartile, median, upper quartile and the largest observation (sample maximum) ($N = 4266$).

Title Page

Abstract

Introduction

Conclusions

References

Tables

Figures

◀

▶

◀

▶

Back

Close

Full Screen / Esc

Printer-friendly Version

Interactive Discussion



Simulations of the transport and deposition of ¹³⁷Cs after Chernobyl

N. Evangeliou et al.

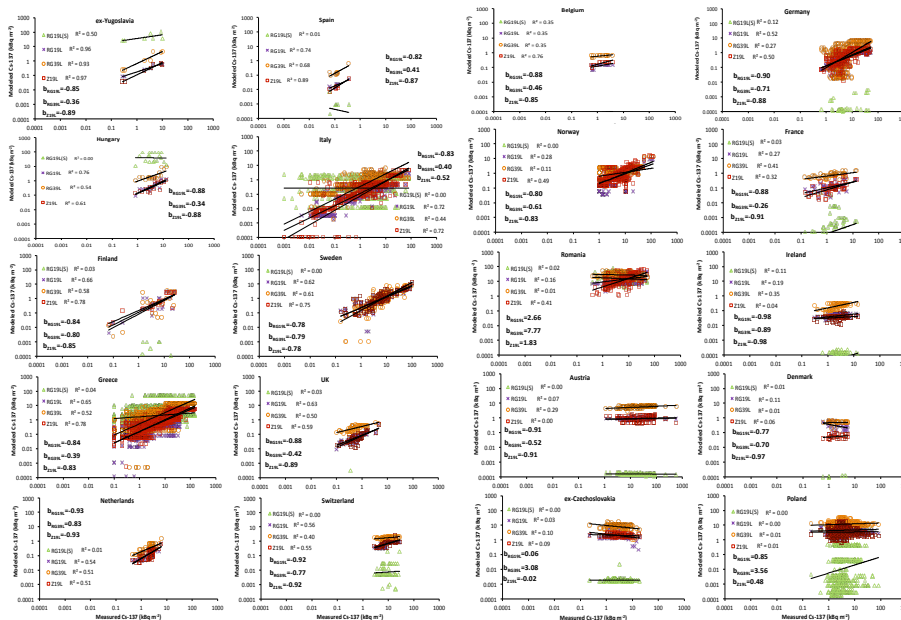


Fig. 20. Linear regression scatter plots of the cumulative deposition of ¹³⁷Cs in 20 European countries from the simulations of all model versions (Modeled Cs-137) and the REM database (Measured Cs-137). The plots are presented in descending order from the best to the worst linear fitting. The estimated biases are also shown for all the runs (b_{RG19L} , b_{RG39L} and b_{Z19L}) except for the one where surface emissions assumed.

Title Page

Abstract

Introduction

Conclusions

References

Tables

Figures

◀

▶

◀

▶

Back

Close

Full Screen / Esc

Printer-friendly Version

Interactive Discussion